AMERICAN SOCIETY of
GENE & CELL
THERAPY

Targeted Cell-to-Cell Delivery of Protein Payloads via the Granzyme-Perforin Pathway

Daniel J. Woodsworth,[1] Lisa Dreolini,[1] Libin Abraham,[2] and Robert A. Holt[1,3,4]

[1]Canada's Michael Smith Genome Sciences Centre, BC Cancer Agency, Vancouver, BC V5Z 1L3, Canada; [2]Department of Microbiology & Immunology, University of British Columbia, Vancouver, BC V6T 1Z3, Canada; [3]Department of Medical Genetics, University of British Columbia, Vancouver, BC V6T 1Z4, Canada; [4]Department of Molecular Biology and Biochemistry, Simon Fraser University, Burnaby, BC V5A 1S6, Canada

There is great potential for engineering cellular therapeutics by repurposing biological systems. Here, we report utilization of the granzyme-perforin pathway of cytotoxic lymphocytes as a cell-to-cell protein delivery module. We designed and constructed granzyme B-derived chaperone molecules fused to a fluorescent protein payload and expressed these constructs in natural killer (NK) cells. Using confocal microscopy and flow cytometry, we investigated the co-localization of the chaperones with lytic granules and the chaperone-mediated transfer of the fluorescent protein payload from NK to target cells in co-culture experiments. A synthetic chaperone consisting of the granzyme B ER signal peptide and a domain encompassing putative N-linked glycosylation sites in granzyme B is insufficient for payload transfer to target cells, whereas full-length granzyme B is sufficient for payload delivery. Combining our functional data with an analysis of the crystal structure of granzyme B suggests that the necessary motifs for granzyme B loading into lytic granules are dispersed throughout the primary amino acid sequence and are only functional when contiguous in the tertiary structure. These results illustrate that by using granzyme B as a molecular chaperone the granzyme-perforin pathway can be exploited as a programmable molecular delivery system for cell-based therapies.

INTRODUCTION

With their ability to sense and integrate a wide range of signals, actively move to specific tissue compartments, and actuate context-dependent responses, engineered cell-based therapeutics are emerging as the next major class of medical intervention.[1] Chimeric antigen receptor T cells (CAR Ts) are highly effective in treating hematological malignancies,[2–4] and many mesenchymal stem cell therapies[5] are at various stages of development for use in cardiac,[6,7] neurological,[8] and malignant[9–11] disease. These advances are a result of recombining the diverse functionality of biological systems to generate new functional biological molecules and pathways.[12,13]

For any useful cellular device, three primary components are required: input modules, control logic, and output modules. Significant progress has been made with the former two, including a variety of transcriptional control circuits[14] as well as highly specific and configurable chimeric antigen receptors[15] and synthetic notch receptors.[16,17] Output modules for cellular devices have been less developed and investigated. Most rely on passive, nonspecific secretion, activated by a combination of sensory input modules, modulated by control circuits.[18] This approach has potential for a variety of metabolic derangements,[19] but also has a significant limitation in that transcriptionally activated secretion creates a temporal delay between activation and actuation. For many applications, an ideal output module would have the deliverable payload pre-positioned for rapid actuation and delivery. Furthermore, secretion only achieves regional specificity at best. In many cases cell-specific delivery would be extremely valuable, both as a research tool, as well as in therapeutic contexts.

To date the most investigated and best understood cell-to-cell delivery systems are bacterial in origin, specifically bacterial type III and type IV secretion systems.[20–22] Other synthetic biology approaches have also been developed using, for example, invasin triggered by environmental signals or quorum sensing.[23,24] These designs achieve cell-specific delivery, yet they retain two major weaknesses. First, they are for the most part transcriptionally controlled, resulting in a lag between activation and delivery, and second, they are bacterial in origin, likely raising prohibitive immunological obstacles to human therapeutic applications.

We set out to develop a cell-to-cell delivery module in which payload delivery could be rapidly initiated by surface receptors, with this activation resulting in the transfer of the payload from the delivery cell to a target cell in a cell-specific manner. Further, we desired that delivery originate from a pre-positioned source, such that the time between initiation of target recognition and completion of payload delivery is a short, tightly coupled process. The granzyme-perforin pathway, in the context of a cytotoxic lymphocyte chassis, is a unique and potentially broadly applicable cell-to-cell delivery system that fulfilled these criteria. This pathway is one of the main ways in which cytotoxic lymphocytes kill target cells.[25] Its main constituent components are the serine protease granzymes and the pore forming protein perforin, both of which are stored in membrane-bound secretory lysosomes, or
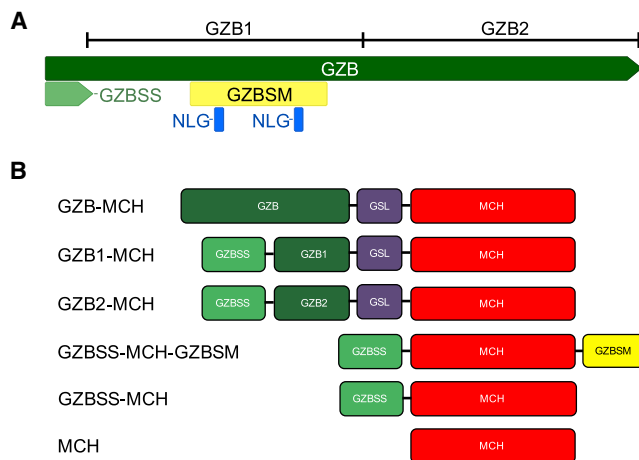
CrossMark

Figure 1. Design of Payload Delivery Module Chaperones

(A) Granzyme B as a model protein that transits the granzyme-perforin pathway. The full-length coding sequence is shown in green, with the ER signal peptide in light green (GZBSS). The two putative N-linked glycosylation motifs are shown in blue (NLG), with the encompassing putative sort motif (GZBSM) in yellow. The boundaries of the first and second halves of granzyme B used in this study (GZB1 and GZB2) are shown above the full-length coding sequence. (B) Schematic of the constructs used in this study. crmCherry (MCH, red), an RFP protein was used as a model payload, and a flexible glycine serine linker (GSL, purple) was used to join GZB, GZB1, and GZB2 to MCH.

lytic granules, in the cytosol of cytotoxic lymphocytes.[26] Upon target cell recognition, the cytotoxic lymphocyte forms a tight apposition with the target cell, forming the immunological synapse. Surface receptor signaling results in the endocytic release of granzymes and perforin from the lytic granules into the synapse between the two cells.[27] Perforin then inserts in the target cell membrane and oligomerizes to form transient pores, through which granzyme diffuses into the target cell.[28–30] Finally, granzyme cleaves caspases and BH3-interacting domain death agonist (BID) to initiate target cell apoptosis. Importantly, surrounding bystander cells typically do not receive appreciable quantities of granzymes.[31–33] In summary, surface receptor-mediated target cell recognition results in specific, cytoplasm-to-cytoplasm intercellular transfer of granzymes to that same target cell. More broadly, cytotoxic lymphocytes have exceptional utility as a cellular chassis because they are targetable, expandable, and amenable to genetic manipulation.[34]

This combination of the granzyme-perforin pathway and cytotoxic lymphocyte chassis fulfill all of the requirements for a cellular device output module listed above: native and engineered targeting modules (T cell receptors or chimeric antigen receptors) that naturally interface with a signaling cascade that initiates release of pre-positioned molecules, that are delivered in a cell-specific manner, as defined by the original surface receptor recognition of the target cell.

Granzyme B (GZB) is a well-studied effector molecule that transits the granzyme-perforin pathway. Here, we engineer granzyme B-derived chaperones and trace chaperone mediated trafficking of a

functional fluorescent protein payload through this pathway from effector to target cells. This demonstrates the implementation of a programmable cell-to-cell transfer module that can potentially be used to deliver different ectopic protein payloads to targeted tissues or cells.

RESULTS

Design of Granzyme B-Derived Molecular Chaperones

Granzyme B is synthesized as a pre-pro-protein, with an 18 amino acid N-terminal endoplasmic reticulum (ER) signal peptide, followed by an inhibitory dipeptide, followed by the rest of the protein.[26] Upon initiation of translation, the ER signal peptide directs the nascent protein to the ER, where it is co-translationally inserted into the ER. As the protein is synthesized in the ER, an N-glycan is added, which targets the protein to the Golgi network once synthesis is complete. In the Golgi, the N-glycan is further phosphorylated. This phosphosugar moiety on granzyme B then binds to the mannose-6-phosphate receptor, which targets the protein to lytic granules, where it is sequestered until target cell recognition, resulting in granzyme B release into the immune synapse.[27] Importantly, recent work has shown that following release into the immune synapse, the trafficking of granzyme B to the target cell membrane and entry into the target cell via perforin pores is likely a result of passive diffusion only.[28,29,33]

We used this information to guide our design of chaperones for granzyme-perforin-mediated delivery. Since the steps in this process that are downstream of lytic granule exocytosis appear to be passive, we hypothesized that a chaperone that successfully directed a payload to be loaded into lytic granules would also be sufficient for payload delivery to the target cell. In designing such a chaperone, we adopted two strategies: rational and empirical (schematics for all constructs used in this paper are found in Figure 1).

For our rational design, we sought to develop a set of minimal granzyme B domains that would shuttle a protein payload to lytic granules. We took this set to be an ER localization domain and a lytic granule localization domain. For the former, we used the granzyme B ER signal peptide (GZBSS). For the latter, we used a 53 amino acid motif surrounding two computationally predicted N-linked glycosylation sites (GZBSM). Our final rational design consisted of GZBSS at the N terminus, followed by the model payload, followed by GZBSM. For a model payload, we selected crmCherry (hereafter mCherry or MCH), a derivative of the mCherry red fluorescent protein that is known to be stable in the acidic environment of lysosomes.[35]

The behavior of chimeric proteins consisting of domains derived from multiple proteins that have been rearranged is unpredictable. Therefore, we also selected full-length granzyme B as an empirical chaperone. Our rationale for this choice was that if there were unknown domains within granzyme B other than the region surrounding the N-linked glycosylation sites that were necessary for lytic granule loading or if the necessary domains are adjacent to the N-linked glycosylation sites only in the tertiary structure of granzyme B, then they

would be captured in the full-length protein. As a first step toward delineating the location of these critical motifs within full-length granzyme B, we also investigated the first and second halves of granzyme B (GZB1 and GZB2, respectively) as independent chaperones. If either of these halves were functional as a chaperone, not only would it indicate that a minimal motif was present in them, from a practical standpoint this would be useful as it would yield a smaller chaperone, potentially much smaller if the process were repeated and the minimal motif further constrained. We placed the GZBSS ER signal peptide at the N terminus of both GZB1 and GZB2. To keep these granzyme B domains in as native a form as possible, we fused the MCH payload to the C terminus of GZB, with the two proteins connected by a flexible glycine serine linker.

As controls, we also generated two additional constructs: MCH alone and GZBSS followed by MCH.

Screening Chaperone Designs by Assessing Lytic Granule Co-localization Using Confocal Microscopy

Since our hypothesis was that lytic granule loading of a payload would be sufficient for payload delivery, we first investigated the subcellular localization of the chaperones using confocal microscopy. Using electroporation, we expressed the candidates in the natural killer cell line YT-Indy, which retains a functional granzyme-perforin pathway and has well-characterized target cell lines.[36] Following enrichment for mCherry^{+} cells via cell sorting, we stained the cells for the lysosomal and lytic granule marker Lamp1 and then acquired images of the cells using confocal microscopy. As expected, the Lamp1 distribution was punctate in nature, but the MCH distribution was highly variable (Figure 2).

Due to the range of phenotypes observed in the images, we sought to evaluate the degree of payload (MCH) co-localization with Lamp1 in an unbiased manner. To do this, we developed a semi-automated image filtration and analysis pipeline. The algorithm is illustrated in Figure 3 and seeks to eliminate both local background and bleed as well as pixel noise. This is achieved using both local and global image information to filter each pixel. This filtering is critical to enable quantitation of co-localization, as it eliminates the background noise from the regions of the image in which there are no cells, as well as regions that are adjacent to granules that have moderate signal intensity, both of which could give a spurious contribution to any quantitative metric of co-localization. The efficacy of this method can be observed by examining the progression of the columns from top to bottom of Figure 3: note that pixel intensities of the punctate structures remain relatively intact, whereas the binarized images (showing the extent of the background signal) change from containing large homogeneous structures to puncta that closely resemble those in the pixel intensity images. To our knowledge, this combination of local background subtraction with global pixel noise filtration has not been reported previously. We feel that it is particularly useful for studies involving small, subcellular structures, and in the hopes that it will be of use to the community, we have included the source code that implements the algorithm in the Supplemental Information.

Using this approach, we quantified the co-localization between MCH and Lamp1 in these filtered images using the Manders M1 coefficient and Pearson correlation coefficient (PCC) (Figure 4). Both metrics indicated that MCH alone had a low degree of co-localization with lytic granules, which would be expected as the lytic granules are small dense granules, and unfused MCH is distributed throughout the cytosol. These quantitative metrics were less useful for differentiating between the remaining fusion proteins. This motivated us to qualitatively assess the morphology of the distributions of MCH and Lamp1 and use this as a guide to selecting candidate chaperones. GZBSS-MCH had a perinuclear and membrane distribution, consistent with it entering the secretory pathway. GZB-MCH displayed a punctate cytosolic distribution consistent with granule loading. GZBSS-MCH-GZBSM exhibits a heterogeneous distribution that is partially punctate and granular (similar to GZB-MCH) and partially of moderate intensity, diffuse, and cytosolic (similar to unfused MCH). GZB1-MCH has an interesting membranous phenotype, which we hypothesize might be a result of this fusion protein entering the secretory pathway. GZB2-MCH has a highly punctuate distribution, but one that is considerably divergent from that of the Lamp1 distribution. The marked difference in the morphology of the subcellular localization of the two halves of granzyme B is interesting, and we discuss this further below. In summary, our assessment of the subcellular distribution of the various chaperone mCherry fusion proteins led us to conclude that GZB-MCH and GZBSS-MCH-GZBSM had the most potential as candidate chaperones.

Transfer of Fusion Proteins from Effector to Target Cells

We next characterized the capacity of two candidate chaperones (GZBSS-MCH and GZBSS-MCH-GZBSM) to facilitate transfer of the payload through the granzyme perforin pathway to target cells. To do this, we conducted a series of co-culture experiments, again using mCherry as a fluorescent reporter payload that was easily traceable. Effectors expressing a variety of mCherry fusion proteins were co-cultured with fluorescently labeled target cells, and then analyzed for evidence of mCherry in the target cell populations. We used the B cell lymphoblastoid cell line 721.221 (hereafter 721)[37] as target cells, as they are a well known YT-Indy target.

We started by testing GZB-MCH, GZBSS-MCH, and MCH alone. GZB-MCH was the chaperone our microscopy images had suggested was most likely to load payloads into lytic granules, while MCH alone was clearly not loaded into lytic granules and thus a good control. GZBSS-MCH was included to confirm that it was not being loaded into lytic granules and hence would not be transferred to target cells. YT-Indy cells were transfected with plasmids coding for these chaperones and then FACS enriched for RFP^{+} cells. The various effector cell types were separately co-cultured with 721 target cells that had been labeled with a fluorescent dye, to distinguish between the effector and target cells. This mixed cell population was then analyzed via flow cytometry (Figure 5). Target 721 cells that were co-cultured with YT-Indys expressing GZB-MCH show an increase in mCherry signal, as compared to 721 s alone, 721 s co-cultured with unmodified YT-Indys, and 721 s co-cultured with YT-Indys expressing either
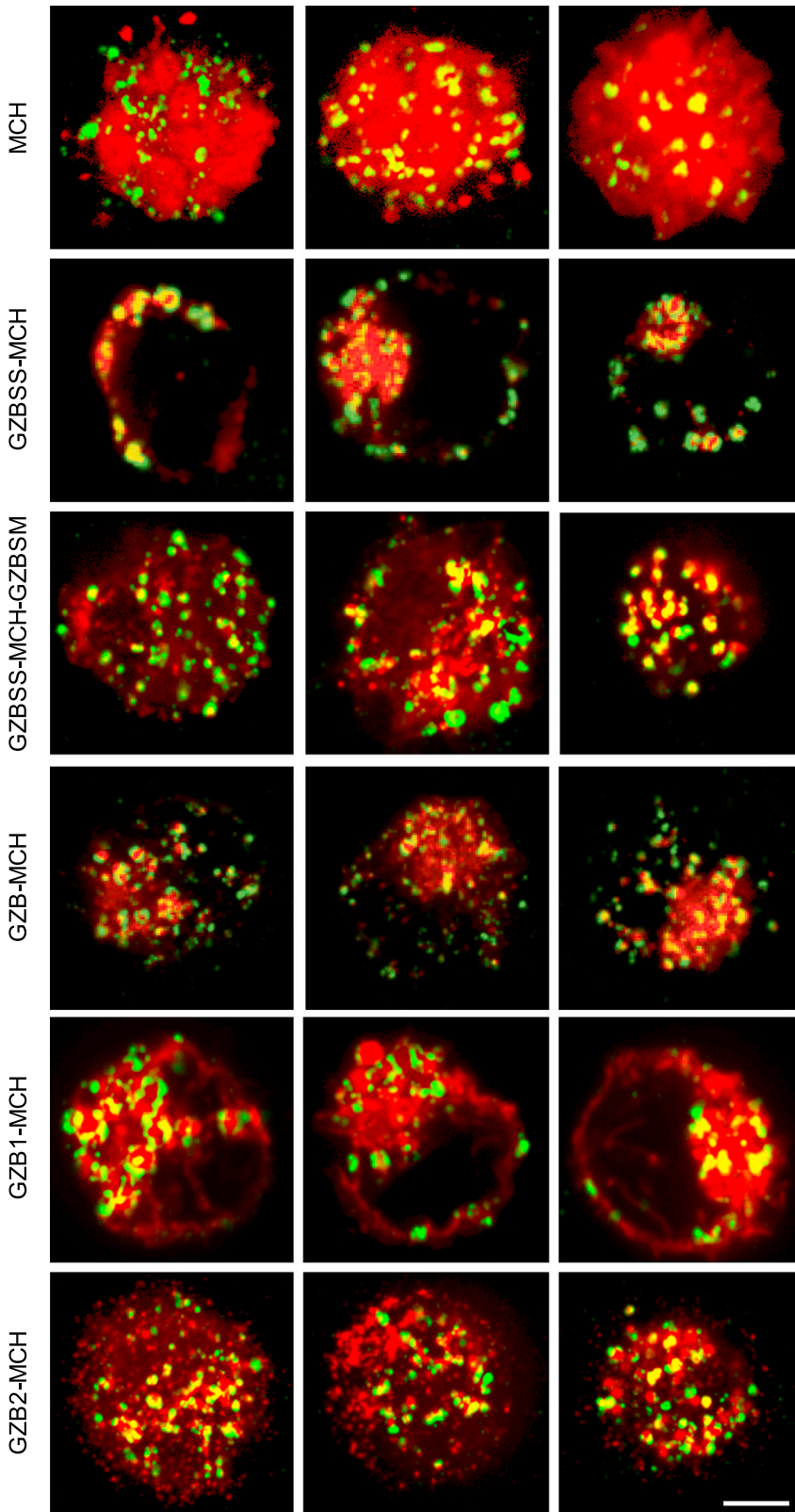
Figure 2. Subcellular Distribution of Candidate Chaperone-mCherry Fusion Proteins

YT-Indys expressing the candidate fusion proteins (labeled at left) were stained for the lytic granule marker Lamp1 and imaged using confocal microscopy. Shown are merged red (mCherry) and green (Lamp1) channels for three representative cells for each sample. White scale bar, 5 μm.
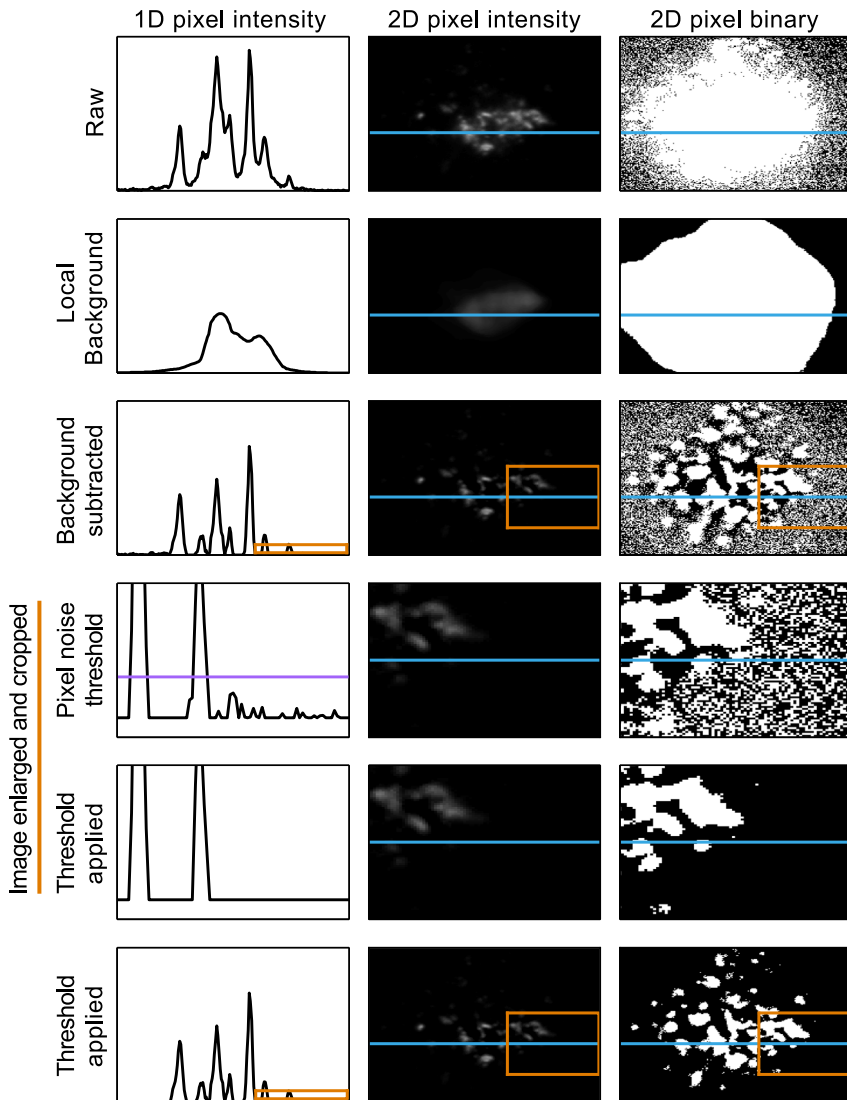
Figure 3. Automated Image Noise Filtering Pipeline

All panels are derived from a single channel of a single image. The first column consists of pixel intensity traces of a single horizontal line of pixels from the corresponding two-dimensional image in the second column (this line is shown in blue throughout the figure). The third column shows binarized versions of the middle column: all pixels with intensity greater than 0 are set to 1. The first row is the raw image data. The second row is the local background of the image. The third row is the background subtracted image, literally the second row subtracted from the first. The section of the images enclosed by the orange boxes in the third row have been enlarged and are displayed in the fourth row, to better show the pixel noise (small fluctuations near zero in the first column). The horizontal purple line is the threshold that will be applied to filter pixel noise. The fifth row shows the final resulting image after the threshold has been applied. The bottom row also shows the final processed image but zoomed back out to allow for comparison to rows 1–3. As in row 3, the orange boxes correspond to the region enlarged in rows 4 and 5.

mCherry signal in target cells and mCherry signal in target cells resulting from chaperone-mediated transfer. The data (Figure 6) are consistent with our initial co-culture experiments and indicate that GZB transfers MCH to target cells, but GZBSS or GZBSS in combination with GZBSM does not. The fact that GZBSS-MCH-GZBSM did not transfer MCH to target cells is interesting. Given the mixed phenotype observed in YT-Indys expressing this construct in our microscopy images, we thought there was a possibility that it might also traffic to target cells. The fact that it does not provides useful information concerning the nature and location of the granzyme B motifs responsible for its trafficking through the granzyme-perforin pathway, which we discuss below.

MCH or GZBSS-MCH. Notably, this increase is most prominent in the dead cell fraction (DAPI+) of the target cells. Since the majority of these cells are dying due to YT-Indy attack, DAPI positivity can be viewed as a proxy for YT-Indy targeting. Therefore, the increase in MCH signal in dead (DAPI+) targets co-cultured with YT-Indys expressing GZB-MCH, but not MCH or GZBSS-MCH, suggests that GZB-MCH is transferred to target cells specifically via chaperone-mediated trafficking through the granzyme-perforin pathway.

We then investigated if the rationally designed chaperone (GZBSS-MCH-GZBSM) would perform similarly to GZB-MCH. We conducted the same type of experiment as above, comparing YT-Indys expressing GZBSS-MCH, GZBSS-MCH-GZBSM, and GZB-MCH. We selected GZBSS as the comparator so that all constructs would have the same N-terminal ER signal peptide and potential for secretion. This would allow us to differentiate between non-specific

Finally, to confirm at the protein level that granzyme B transfers the MCH payload to target cells, we repeated the above experiments, with the additional, post-co-culture, step of collecting live and dead (DAPI− and DAPI+, respectively) 721 target cells from each co-culture via fluorescence-activated cell sorting (FACS). Data from this sort is shown in Figure 7A, and it is consistent with the flow cytometry data from our other experiments. Whole-cell lysates from the sorted target cell populations were then size-separated by gel electrophoresis and probed for mCherry via western blot (Figure 7B). A prominent 60-kDa band consistent with GZB-MCH is observed in lysates of 721s co-cultured with YT-Indys expressing GZB-MCH. There is also a background band of approximately 30 kDa, consistent with unfused mCherry in the lysate of 721s co-cultured with YT-Indys expressing GZBSS-MCH. This is not unexpected, as the ER signal peptide in GZBSS-MCH directs mCherry to the secretory pathway,[38] resulting in extracellular mCherry, some of which is likely taken up by
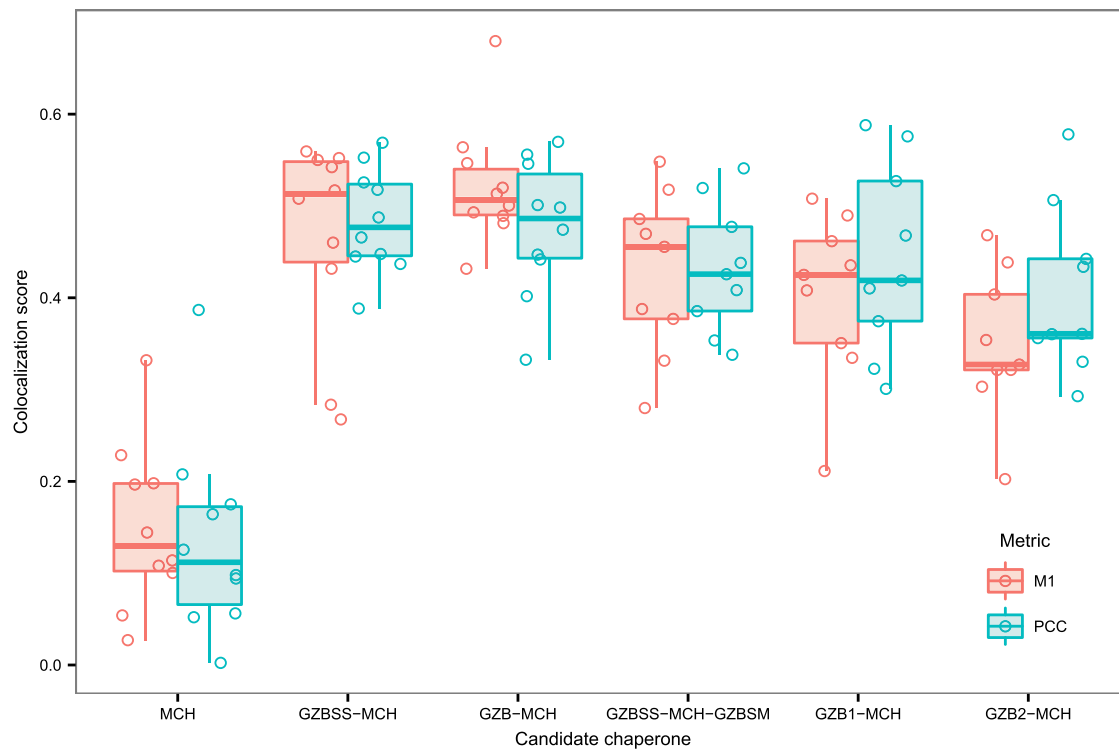
Figure 4. Quantitative Assessment of Candidate Chaperone Co-localization with Lytic Granules

Two co-localization metrics were calculated: Manders M1 (quantifying the fraction of pixel intensity of mCherry-positive pixels that also contain Lamp1 signal) and Pearson correlation coefficient (PCC, quantifying the degree to which red and green pixel intensities are correlated). These were calculated using both channels from each image. Each circle is the score of a single image, and each image contained between two and five cells. Overlaid are box and whisker plots.

the target 721s. However, if non-specific uptake were the main mechanism of MCH transfer from effector to target cell for all samples, then we would not expect to see any difference between 721s co-cultured with YT-Indys expressing GZB-MCH compared to 721s co-cultured with YT-Indys expressing GZBSS-MCH. Instead, of the DAPI$^+$ 721 samples, only the sample from targets that were co-cultured with YT-Indys expressing GZB-MCH has detectable amounts of mCherry protein, and this band is detected at approximately 60 kDa, the expected size of GZB-MCH. Conversely, there is no detectable analogous 30-kDa band corresponding to MCH in the lysates from DAPI$^+$ targets co-cultured with YT-Indys expressing GZBSS-MCH. That the putative GZB-MCH band in the DAPI$^+$ 721 sample co-cultured with YT-Indys expressing GZB-MCH is even detectable is noteworthy given the actual amount of protein loaded is quite small, as demonstrated by the lack of a vinculin-loading control band. This is despite equal cell numbers for all lanes being sorted and lysed and is because the DAPI$^+$ dead cells are apoptotic and rapidly degrading, which results in a loss of protein.

Taken together, these results and analysis suggest that while there is some background, non-specific 721 uptake of MCH from the co-culture media, YT-Indys expressing GZB-MCH specifically transfer the fusion protein to targeted 721s, while YT-Indys expressing GZBSS-MCH and GZBSS-MCH-GZBSM do not specifically transfer MCH

to targeted 721s. Thus, granzyme B appears to be a suitable chaperone protein for delivery of protein payloads via the granzyme-perforin pathway.

DISCUSSION

Cellular therapeutics that repurpose and recombine biological function in a cellular chassis are transforming medicine.[1] These efforts will rely heavily on the development of modules and systems that perform specific sensory, computational, and effector functions.[12,13] We report here our efforts to develop a cell-to-cell delivery module for cellular therapeutics by repurposing the granzyme-perforin pathway of cytotoxic lymphocytes. Our results support the use of granzyme B as a molecular chaperone for inserting protein payloads into this pathway and facilitating payload delivery to target cells.

We hypothesized that lytic granule loading of a payload would be sufficient for transfer to a target cell, and that loading could be achieved by fusing a chaperone to the payload. We designed two candidate chaperones derived from granzyme B, fused them to mCherry, and investigated their subcellular localization in the natural killer cell line YT-Indy.

All constructs containing an N-terminal ER signal peptide exhibited a high degree of co-localization with Lamp1, as opposed to MCH alone.
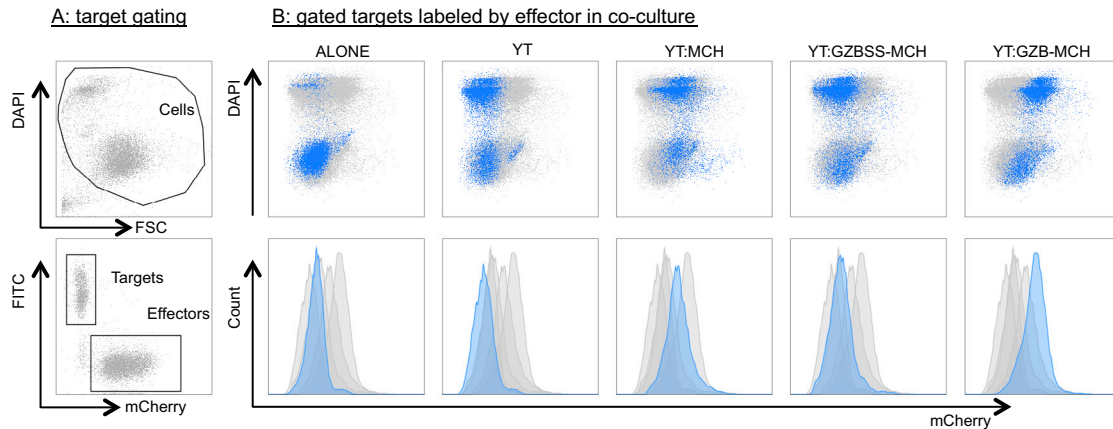
Figure 5. Transfer of Granzyme B mCherry Fusion Protein to Target Cells

YT-Indys expressing various mCherry fusion proteins were co-cultured with CFSE-labeled target 721 cells, and the mixed population was analyzed via flow cytometry. (A) Gating strategy for isolating target cells. Debris was eliminated (top panel), and then FITC⁺ targets selected (bottom panel). Not shown is an intermediate hierarchical gating step in which doublets are excluded using forward and side scatter width versus height gates. (B) Target 721 cell mCherry fluorescence. Each column is labeled by the effector that was present in the co-culture, but only target cells are plotted, using the gating from (A). Each column contains the same data showing target cell populations from all co-cultures, but only a single target population is highlighted in blue, which corresponds to the effector partner that was present in the co-culture partner.

This result is best understood by considering the biological distribution of Lamp1 and the cellular compartments in which the co-localization occurs. The primary route of newly synthesized Lamp1 follows the secretory pathway to exosomes at the cell membrane and is then recaptured in early endosomes and eventually fuses with nascent lysosomes.[38,39] In the case of GZBSS-MCH, the ER signal peptide would direct the protein to the secretory pathway, so GZBSS-MCH is expected to be found co-localized with Lamp1 in a perinuclear distribution in the ER and Golgi and in punctate granules at the cell membrane, but not in cytoplasmic lytic granules. This is what we observe in cells expressing GZBSS-MCH, in contrast to those expressing GZB-MCH, in which the observed co-localization is primarily in cytoplasmic puncta, consistent with lytic granules. These observations are supported by our co-culture experiments, which indicated that GZB-MCH was transferred from effector to target cell, but not GZBSS-MCH. This interpretation is predicated on the assumption that entry into the target cell via perforin pores is passive, which, while historically controversial, is supported by most recent experimental and theoretical data.[26,28,29,33,40]

We postulated that combining an ER signal peptide with a putative N-linked glycosylation motif would be sufficient for payload delivery, but our co-culture results clearly refuted this. That GZBSS-MCH-GZBSM did not transfer to target cells has several interesting implications surrounding the intracellular trafficking of granzyme B. The first is that the putative N-linked glycosylation sites we computationally identified and their flanking amino acids are insufficient for granule loading. While we cannot rigorously exclude the possibility, we do not believe that these results are simply due to faulty glycosylation of GZBSM, since this process occurs co-translationally and only depends on local sequence.[41] This suggests then that GZBSM is not being phosphorylated, likely because

the binding domain for the GlcNAc-1-phosphotransferase, which adds a phosphate group to the mannose of the N-linked glycan in the Golgi,[38] is not faithfully recapitulated in GZBSS-MCH-GZBSM. This could either be due to a lack of actual amino acids that are present elsewhere in the full-length granzyme B protein or that the phosphotransferase-binding domain is conformation dependent, as has been suggested elsewhere in the literature,[42] or both. Much work has been invested into characterizing this domain, but its exact nature remains elusive. Our results suggest that whatever the exact composition, its constituent residues are likely distributed throughout the primary amino acid sequence and hence were not captured in GZBSM, which is why it failed to facilitate transfer of the MCH payload to target cells. This conclusion is consistent with the location of the asparagine residues within the context of GZBSM and the full-length granzyme B protein. As shown in Figure 8, both of the N-linked glycosylation sites we computationally identified are located immediately adjacent to residues that lie external to GZBSM. In particular, N104 is located at a junction in which residues on one side of N104 are located within GZBSM, while those on the other side are located in the other half of the granzyme B protein (Figures 8A and 8C). Also of note is that the other N-linked glycosylation site (N71) is surrounded by a triangular pattern of lysines (Figure 8D), a pattern which some experimental data suggests is the phosphotransferase binding site.[43,44]

The conclusion that the domains necessary for lytic granule (LG) loading lie throughout the granzyme protein is further supported by our microscopy data, which showed that neither half of granzyme B co-localized with Lamp1 in a similar fashion to full-length granzyme B. This data is also consistent with the arginine residue structural analysis presented above. Beyond corroboration, the
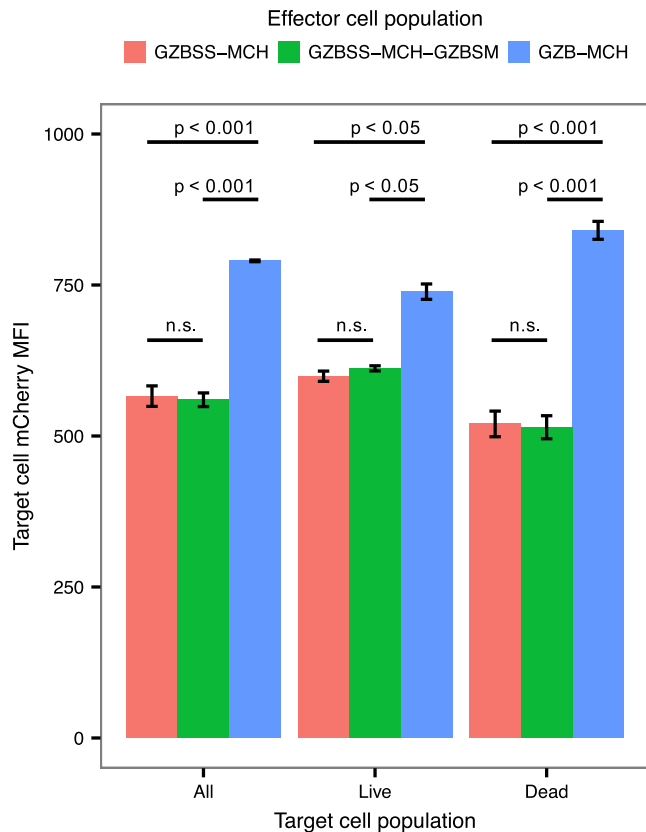
Figure 6. Comparison of MCH Payload Transfer to Target Cells by the Two Granzyme B-Derived Chaperones

YT-Indys expressing GZBSS-MCH (red), GZBSS-MCH-GZBSM (green), or GZB-MCH (blue) fusion proteins were co-cultured with CFSE-labeled target 721 cells, and the mixed population was analyzed via flow cytometry. The same gating strategy from Figure 5 was used, and only target cells are plotted. Live and dead cells were selected using a DAPI versus MCH dot plot. Bar plots show mean fluorescent intensity of the RFP channel (MCH MFI) of 721 target cells, with error bars denoting the standard deviation of duplicate samples. p values were calculated using Tukey's HSD test applied to the results of a single factor ANOVA that was conducted for each target cell population separately.

morophological appearances of GZB1-MCH and GZB2-MCH are interesting in their own right. In particular, the membranous distribution of GZB1-MCH suggests it is entering the secretory pathway, similar to GZBSS-MCH, and further suggests that the absence of key domains found in GZB2 are preventing GZB1-MCH from being sorted to LGs. Interpreting the highly punctate distribution of GZB2-MCH that is nevertheless distinct from that of Lamp1 is more challenging. It is possible that the sorting domains found in GZB2—that presumably make up part of the overall complement of domains in full-length granzyme B responsible for its localization to LGS—are degenerate or otherwise used by a variety of sorting pathways in the Golgi. This degeneracy could result in GZB2-MCH being sorted into another, unknown, granular compartment distinct from LGs or other granules containing Lamp1. However, this is speculative and would require experimental investigation.

In summary, our results argue that granzyme B trafficking to lytic granules requires residues or domains beyond those immediately flanking the putative N-linked glycosylation motifs. In particular, this data implies that the GlcNAc-1-phosphotransferase binding domain is not a contiguous amino acid sequence, but rather a conformation-dependent motif composed of residues located throughout the length granzyme B. By extension, this analysis and data suggest that barring fine-scale delineation of the exact residues and three-dimensional motifs necessary for LG loading, using full-length granzyme B will likely be necessary for delivery of a payload to a target cell, at least in the near term. Both the flow cytometry and western blot data from our co-culture experiments demonstrated that it is also sufficient: YT-Indys expressing GZB-MCH transfer it to 721 target cells. Importantly, these same data also indicated a background level of accumulation of mCherry signal in target cells co-cultured with YT-Indy cells expressing the comparator constructs (GZBSS-MCH and MCH alone). While this might initially appear to undermine the utility of this system, we in fact believe the opposite: it demonstrates the need for specific, cell-to-cell delivery, the activation of which is controlled by surface receptor interactions. In the case of comparator effector populations expressing GZBSS-MCH or MCH, the mCherry signal is the same in both live and dead target cells, indicating a non-specific effect. If these effector cells were used to deliver the payload, the specificity of delivery would be at best localized. However, in the case of the GZB-MCH-expressing effector population, there is a significant increase in the RFP signal in dead target cells, indicating that YT-Indy-targeted 721s specifically received the most GZB-MCH. Furthermore, our observations consistently have been that MCH is much brighter than GZBSS-MCH, which is in turn brighter than GZB-MCH. If the transfer were non-specific and occurred at roughly equal rates for all mCherry fusion proteins, then we would expect to see 721s cocultured with YT-Indys expressing MCH alone to display the greatest increase in RFP signal, followed by those co-cultured with GZBSS-MCH and finally those with GZB-MCH. Instead, we see the opposite: with the greatest increase in RFP signal in cells co-cultured with YT-Indys expressing GZB-MCH, despite this fusion protein having the dimmest fluorescent intensity. Together, this data suggests there is a basal level of background accumulation of the mCherry payload in all cases, but substantial, target-specific transfer of the payload in the case of YT-Indys expressing GZB-MCH.

The successful transfer of GZB-MCH highlights two unique and highly desirable features of the granzyme-perforin pathway: modularity and prepositioning. The first is important in that all that is required to deliver a payload is to fuse it to the chaperone. In principle, no further modifications are required, regardless of the payload. This modularity suggests that the system might be widely applicable as a means of cellular delivery, either in cytotoxic lymphocytes, or in the long term, in other, orthogonal, highly engineered cellular chassis. The second advantage is that, as opposed to producing a payload in response to target cell recognition using transcriptional control, a pre-synthesized payload loaded into a lytic granule can be released
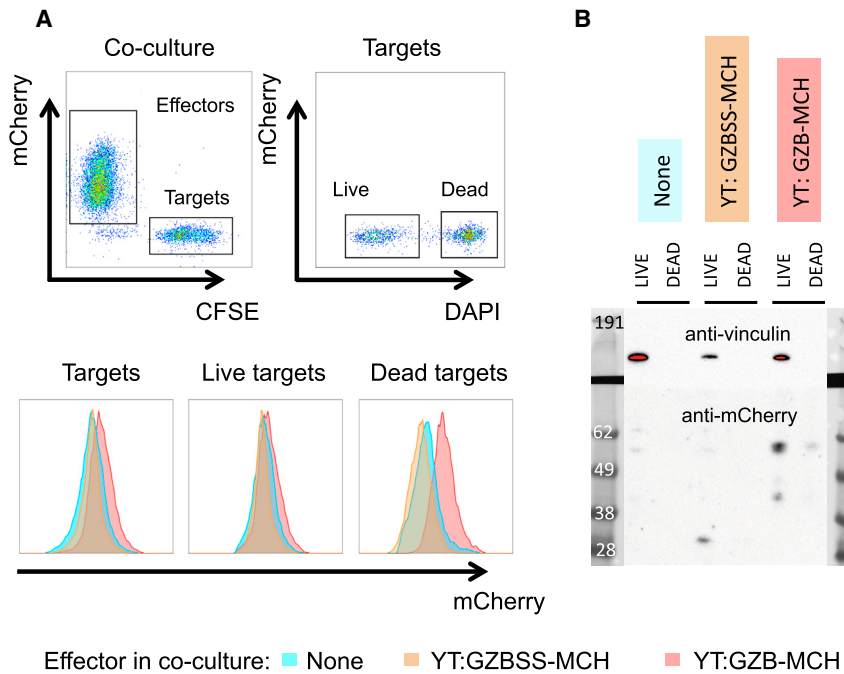
A

B

Figure 7. Western Blot Confirmation of GZB-MCH Fusion Protein Transfer to Target Cells

(A) FACS sort data. YT-Indys expressing either GZB-MCH or GZBSS-MCH were co-cultured with CFSE-labeled target 721 cells, stained with DAPI, and FACS sorted. Target cells were first selected (upper left panel) and then divided into live and dead (upper right), which were sorted separately and analyzed in (B). The bottom panel shows the mCherry fluorescence of targets (bottom left), live targets (bottom middle), and dead targets (bottom right), for 721s co-cultured alone (blue), with YT-Indys expressing GZBSS-MCH (orange), or co-cultured with YT-Indys expressing GZB-MCH (red). (B) Western blot of sorted target cell populations from (A). Equal cell-equivalent amounts of whole-cell lysates of sorted target 721 populations were separated by gel electrophoresis, transferred to blots, and probed for mCherry and vinculin (as a loading control). Note that there is a faint, non-specific background band at roughly 60 kDa in all live lanes. This band is not specific for MCH, and we have observed it across a variety of cell lines from various lineages. It is not visible in the dead lanes simply due to the low amount of protein in these lanes, as discussed in the main text. Expected protein sizes: MCH = 30 kDa; GZB-MCH = 60 kDa; vinculin = 130 kDa. Numbers displayed are sizes in kDa of the protein ladder.

on the timescale during which the immune synapse remains intact, and hence cell-to-cell specificity is maintained.

A critical consideration in using this system is the design and construction of functional fusion proteins that traffic the pathway and remain functional in the target cell. Several issues bear discussion in this regard. Future payloads may not be stable in the harsh environment of the lytic granule, which is acidic and contains many proteases. This might limit the range of applications such a system could be used for, although it is possible that the payload could be engineered to increase its ability to survive the lytic granule, for example by removing a protease cleavage site. The size of the payload is also important, since the internal lumen of the perforin pore has been observed to be 10–20 nm,[28] which sets an upper limit on the payload size. However, the diameter of granzyme B is only 5 nm,[45] leaving an appreciable window for a variety of payloads. The diffusivity of the fusion protein is important to consider, as this dictates the propensity for the granzyme fusion protein to both spread throughout the synapse, translocate through the pore, and escape the synapse.[33] While empirical measurement of the fusion protein diffusivity would be a substantial undertaking, we can at least make estimates regarding the change in diffusivity using the Stokes-Einstein relationship, in which the diffusivity D, is proportional to the inverse of the radius r of the molecule. (The exact relationship is $D = K_B T/(6\pi\eta r)$, where $K_B T$ is the thermal energy and η is the solvent viscosity. Note that aside from r, all other terms are constants between different proteins). The radius of granzyme B and mCherry have both been experimentally determined to be approximately 2.5 nm. Thus, the radius of the fusion protein could be expected to be approximately the average of its long and short dimensions (that is 2.5 and 5 nm), or 3.25 nm. Thus, the ratio

of the radius of the fusion protein to wild-type granzyme is approximately 1.3. Therefore, using the Stokes-Einstein relationship, we would predict that the diffusivity of the fusion protein would be approximately 77% that of the wild-type granzyme. Of course, this analysis only considers the size of the protein and ignores any residue-specific protein-protein interactions, intraprotein effects, effects on solubility, and many other factors. We have conducted a computational study of some of these factors and have found that the rate of perforin pore formation is by far the most important factor in determining the efficacy of granzyme B internalization.[33] Finally, the effect of each fusion partner on the other's function is an important consideration. We have attempted to mitigate this by joining the two by a flexible glycine-serine linker, this has proven successful in maintaining the function of a variety of payloads fused to granzyme B (data not shown). However, in the absence of reliable computational prediction of protein structure and function, the function of both granzyme and the payload of each new fusion would have to be empirically validated, although we note that as more fusions are generated, design rules may become apparent.

As currently implemented, this approach relies upon using a cytotoxic lymphocyte chassis as the delivery cell. Therefore, any eventual application would have to consider the native cytotoxic effector mechanisms of the lymphocyte chassis. Unmodified cytotoxic lymphocytes are appropriate vehicles to deliver payloads to target cells with the intent of killing them, as would be the case with tumor cells. However, for other applications—for example delivery of pro-survival factors in degenerative diseases, deficient enzymes in metabolic diseases, reprogramming cells, or delivery of gene-editing tools in research contexts—the granzyme-perforin delivery functionality
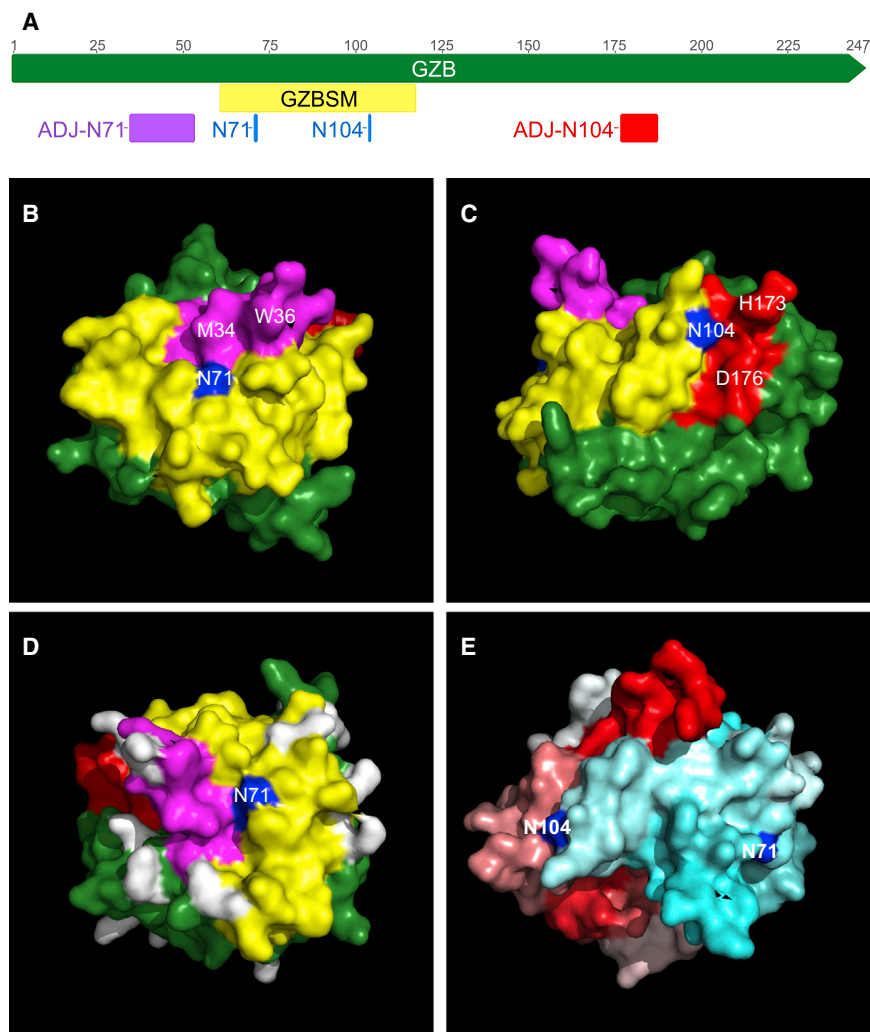
Figure 8. Spatial Context of Putative N-linked Glycosylation Sites in Granzyme B

(A) Schematic of primary amino acid structure of granzyme B. The coloring corresponds to the crystal structures below. Numbers are amino acid residues. (B and C) Three-dimensional crystal structure of granzyme B, colored as in (A), highlighting the potential importance of surface-exposed residues that are immediately adjacent (B, ADJ-N71, purple ; C, ADJ-N104, red) to the N-linked glycosylation sites (blue), but are not contained within the GZBSM (yellow). Note that these regions are quite far from the GZBSM in primary amino acid space, as shown in (A), and in (B) and (C) by the labeling of representative amino acids in these regions. (D) Lysines have been colored in white, to show their inverted triangular pattern surrounding the N71 putative glycosylation site. (E) Location of putative N-linked glycosylation sites (blue) throughout the protein. The residues have been colored from red through white, to cyan, according to their position in the primary amino acid sequence.

transfer of arbitrary payloads with single-cell precision, this system is an important addition to the part set of synthetic immunology.

MATERIALS AND METHODS
Computational Identification of N-Linked Glycosylation Motifs

The granzyme B coding sequence was downloaded from NCBI RefSeq gene (NCBI: NG_028340.1). We then used NetNGlyc 1.0[48] to predict putative N-linked glycosylation sites, of which there were two, 33 residues apart. Since the NX(S/T) consensus sequence is necessary but insufficient for glycosylation and the glycosylation occurs co-translationally,[49] it follows that local sequence context surrounding the consensus site is critical. Therefore, we extracted a 53-amino acid domain from granzyme B, extending from 10 amino acids N-terminal of the first putative glycosylation site, to 10 amino acids C-terminal of the second site. Intriguingly, this domain was also present in human granzyme H.

Plasmids

A custom mammalian expression vector was used in this work (Figure S1). This pdL vector was constructed in house, based on a pcDNA3.1(+) (Thermo Fisher Scientific) backbone. Specifically, the mammalian and bacterial selectable markers and all origins of replication are derived from pcDNA3.1(+), corresponding to bases 1670 (CGATTTCGGCCTATTGGTTA…) to 5396 (…TAAACAAATAG GGGTTCCGC). A custom expression cassette was cloned into this backbone. This cassette consisted of eukaryotic and prokaryotic promoters and ribosomal binding sequences, followed by the open reading frame, followed by eukaryotic and prokaryotic transcriptional termination sites. For the mammalian promoter, we used the CAG

would have to be decoupled from the delivery cell cytotoxicity. This may be possible either through attenuation or knockout of the native effector mechanisms in a cytotoxic lymphocyte or by reconstituting the pathway in an independent, non-cytolytic cell chassis. While both of these suggestions would be challenging undertakings, there have been some remarkable successes in similar endeavors, most notably the reconstitution of basic T cell receptor signaling.[46] The granzyme chaperone itself should be readily catalytically inactivated, as has been previously reported.[47] Alternatively, other classes of chaperone could be considered. Promising candidates include other lytic granule constituents, such as other granzymes and the cathepsins, as well as derivatives thereof. However, we feel strongly that even if all of these approaches were found to be intractable, this system warrants further investigation as a potential therapeutic modality in the context of CAR T cell therapy for cancer.

We have repurposed the granzyme-perforin pathway as a cell-to-cell delivery module for cellular therapeutics. By facilitating targeted

promoter for its ability to drive high levels of expression in a variety of tissues. The sequence was amplified from pEMS1157.[50] This was followed by a hybrid T7 prokaryotic promoter, taken from pCMVTnT (Promega). This was followed by consensus Shine-Dalgarno and Kozak sequences. Following this is the open reading frame, which varies by plasmid. Following the end of the coding sequence, there is a BGH poly(A) sequence, and then a T7 terminator (with both sequences taken from pcDNA3.1(+)). Restriction enzyme cleavage sites flank all components to facilitate subcloning.

The full plasmid sequence for the base pdL vector is in the Supplemental Information, along with the full coding sequence for all plasmids used. All plasmids were constructed through a combination of PCR, synthesis, and restriction/ligation cloning. All PCR amplicons and coding sequences were sequence verified.

Cell Culture

YT-Indy and 721.221 cells were a gift from Judy Lieberman (Harvard University). YT-Indy cells were cultured in RPMI 1640 media, supplemented with 20% heat inactivated fetal bovine serum, 1× GlutaMAX, 1 mM sodium pyruvate, 10 mM HEPES, 0.1 mM beta-mercaptoethanol. 721 cells were cultured in DMEM, supplemented with 10% heat inactivated fetal bovine serum and 1× GlutaMAX. All cell culture reagents were purchased from Thermo Fisher Scientific.

Transfection

YT-Indy cells were electroporated using the Neon system (Thermo Fisher Scientific), using the 100 μL tip. 6×10^6 cells were washed once in PBS, and resuspended in Buffer R along with 20 μg plasmid DNA, in a final volume of 110 μL. The extra volume ensures no bubbles are generated in aspirating the cell mixture into the electroporation tip. Critically, the plasmid DNA must be of a concentration of at least 1 μg/μL, and it must be prepared using an endotoxin-free method. The quality of the plasmid prep greatly influences the electroporation efficiency as well as the post-electroporation viability. The apparatus was prepared as in the manufacturer's manual, using the E2 electrolytic buffer. The electroporation conditions were 3×10 ms pulses at 1250 V. The electroporated cells were then immediately added to 5 mL media spread across two wells of a 6-well plate.

Flow Cytometry

Cells were harvested and resuspended in PBS supplemented with 10% complete media and 1 μg/mL of DAPI (Sigma) as a viability stain. If cells were to be sorted, they were passed through a 35-μm nylon filter (BD Falcon). Cells were kept on ice and then analyzed on a BD Fortessa II or sorted on either a BD Aria III or Fusion. For sorting, cells were sorted into complete media. In all flow cytometry experiments, two initial gating steps were used. Debris was excluded by excluding cells at the bottom left corner of a propidium iodide (PI) versus FSC-A (forward scatter area) gate. Doublets were excluded using a hierarchical gating scheme: all cells with a wider pulse width signal were excluded first in FSC-W versus FSC-H (forward scatter width versus height) and then SSC-W versus SSC-H (side scatter width versus height). All flow cytometry data was analyzed in FlowJo.

Microscopy

Transfected cells were first FACS sorted for moderate intensity RFP$^+$ cells. 2.5×10^5 cells resuspended in 50 μL complete media (RPMI-1640 supplemented with 10% fetal calf serum, 2 mM glutamine, 1 mM pyruvate, 2 μM 2-mercaptoethanol, 50 U/mL penicillin, and 50 μg/mL streptomycin) were adhered to 0.01% poly-L lysine (Sigma) coated, pre-cleaned 12-mm coverslips (#1.0, Fisherbrand) for 15 min at 37°C. Cells were fixed with 2% paraformaldehyde (Electron Microscopy) for 15 min, washed with PBS, and then permeabilized with 0.1% Triton X-100 (Sigma) for 1 min. Samples were washed with PBS and then blocked in 10% goat serum in PBS (blocking buffer) (Jackson Immunoresearch Labs) for 1 hr. Subsequently, cells were stained with polyclonal mouse anti-Lamp1 primary antibody (Abcam cat. #24170) at 1:250 dilution in blocking buffer for 1 hr. Samples were washed with PBS and then stained with Alexa Fluor 488-conjugated goat anti-mouse secondary antibody (Thermo Fisher Scientific cat. #A-11008) at 1:1,000 dilution in PBS for 45 min. After washing with PBS, coverslips were then mounted on glass microscope slides using Prolong Diamond (Thermo Fisher Scientific) overnight. All steps were completed at room temperature unless otherwise noted.

The following day, samples were imaged using a spinning disk confocal system (3i Intelligent Imaging Innovations) based on an inverted Zeiss Axiovert 200M microscope equipped with 100 NA 1.45 Oil Plan Fluor objective and a QuantEM 512SC Photometrics camera. Ten images were acquired for each sample, with each image containing two to five cells in the field of view. All exposure parameters were kept constant across all samples.

Image Analysis

Image filtering was done using a custom script written in MATLAB. The green channel (Lamp1) was filtered as follows: The localized background of the image was calculated for each pixel as the median intensity of a 25×25 pixel square centered on that pixel. This background pixel intensity was subtracted from the original pixel intensity. Any pixels with negative intensity after this step were set to zero. This step aids in distinguishing small punctate structures from one another. Next, a pixel noise threshold was calculated as follows. First the median absolute deviation (MAD) of all nonzero pixels from the raw image was calculated. From this, the standard deviation of the pixel intensity was approximated as 1.4 times the MAD, which is a reasonable estimate of the pixel noise. Finally, the noise threshold was taken as 6 times this value (that is $6 \times 14 \times MAD$). Any pixels in the background subtracted image whose intensity were below this value were set to zero. The red channel (mCherry) was filtered in the same way, except localized background was not subtracted. The MATLAB script implementing this algorithm is in the Supplemental Information.

Colocalization analysis was also conducted in MATLAB. For paired red and green channel images, with pixel intensities R_{ij} and G_{ij} respectively, PCC was calculated as

$$PCC = \frac{\sum_i \sum_j (R_{ij} - \overline{R})(G_{ij} - \overline{G})}{\sqrt{\sum_i \sum_j (R_{ij} - \overline{R})^2 \sum_i \sum_j (G_{ij} - \overline{G})^2}}, \qquad \text{(Equation 1)}$$

where $\overline{G}$ and $\overline{R}$ are the mean pixel intensities. The Manders M1 coefficient was calculated as

$$M_1 = \frac{\sum_{i,j} c_{ij} R_{ij}}{\sum_{i,j} R_{ij}}, \qquad c_{ij} = \begin{cases} 1, & G_{ij} > 0 \\ 0, & G_{ij} = 0 \end{cases}. \qquad \text{(Equation 2)}$$

These co-localization scores were calculated separately for each sample of each image and then plotted using RStudio.

Cell Labeling
Cells were fluorescently labeled with carboxyfluorescein succinimidyl ester (CFSE; eBioscience) following the manufacturer's protocol, except that only one PBS wash prior to labeling was done and only one media wash after labeling was done.

Co-culture Experiments
YT-Indys were transfected with mCherry fusion proteins, and 48 hr later FACS sorted for viable RFP$^+$ cells. The following day 4×10^5 YT-Indy effector cells were combined with 1×10^5 CFSE-labeled target 721 cells at a 4:1 effector:target (E:T) ratio in a final volume of 500 μL YT-Indy media in 5 mL polystyrene round-bottom tubes (BD Falcon). The cell suspension was gently pelleted by spinning it at $200 \times g$ for 15 s. The tubes were then incubated at 37°C for 90 min, and then prepared for flow cytometry or FACS sorting as above.

Statistical Analysis
mCherry median fluorescent intensity was tabulated for each target cell population using flow cytometry data from above. For each target cell population, a single factor analysis of variance was conducted to determine if the MCH median fluorescent intensity (MFI) means were the same for all effector cell populations using the model MFI $\sim$EffectorPopulation. We then used these results as input for a Tukey's honest significant difference (HSD) test of the difference between sample means within each target cell population. Statistical tests were conducted in R, using the aov and TukeyHSD commands respectively.

Western Blotting
3×10^4 cells were sorted into PBS in microcentrifuge tubes. Cells were kept on ice thereafter. Cells were then pelleted, resuspended in 10 μL PBS, and lysed directly by adding 10 μL 2× Laemmli sample buffer. Samples were incubated at 95°C for 10 min and then stored at −20°C.

For blotting, samples were boiled again at 95°C for 10 min and then loaded onto pre-cast 4%–12% Bis-Tris polyacrylamide gels (Thermo Fisher Scientific). Proteins were size separated by gel electrophoresis by running the gel at 150 V for 75 min. Proteins were transferred to a nitrocellulose membrane using a standard wet transfer at 300 mA for 2 hr.

The blot was cut horizontally at 100 kDa and then was blocked in tris-buffered saline with Tween 20 (TBS-T) with 5% skim milk powder at room temperature for 1 hr and then incubated with primary antibody in sealed pouches at 4°C overnight. The primary antibodies used were rabbit anti-mCherry (Biovision cat. #5993-100) and rabbit anti-vinculin (Abcam cat. #EPR8185) as a loading control. The dilutions were 1:500 (mCherry) with 5% skim milk powder, 1:10,000 (vinculin) with 2% skim milk powder, both in TBS-T. Blots were then washed with TBS-T and incubated with horseradish-peroxidase-conjugated goat anti-rabbit secondary antibody (Santa Cruz Biotechnology cat. #sc-2004) for 1 hr. The dilution was 1:5,000 in TBS-T, with 5% skim milk powder (anti-mCherry) and 2% skim milk powder (anti-Vinculin). Finally, the blots were washed with TBS-T and then developed using Bio-Rad Clarity Western ECL (enhanced chemiluminescence) substrate reagent, following the manufacturer's protocol. Blots were imaged using a Bio-Rad Chemidoc MP Imaging System, with exposure times ranging from 1 to 100 s.

Crystal Structure Analysis
To visualize the location of the various motifs of granzyme B in the three dimensional protein, we downloaded the granzyme B crystal structure from the Protein Data Bank (PDB: 1FQ3) and rendered the base crystal structure and custom annotations using PyMOL (Schroedinger). Surface-exposed residues adjacent to the N-linked glycosylation sites were determined by first selecting all residues that were within 15Å of the glycosylated residue. We then selected the subset of these residues that were surface exposed, using a custom PyMOL script written by Jason Vertrees.

SUPPLEMENTAL INFORMATION
Supplemental Information includes one figure, a base pdL plasmid sequence, coding sequence inserts, and MATLAB source code for image filtering algorithm and can be found with this article online at https://doi.org/10.1016/j.omtm.2017.10.003.

AUTHOR CONTRIBUTIONS

CONFLICTS OF INTEREST
R.A.H. and D.J.W. are listed as inventors on a patent application (WO2015157864A1) that covers some of the work presented in this manuscript.

REFERENCES

1. Fischbach, M.A., Bluestone, J.A., and Lim, W.A. (2013). Cell-based therapeutics: the next pillar of medicine. Sci. Transl. Med. 5, 179ps7.

2. Maude, S.L., Frey, N., Shaw, P.A., Aplenc, R., Barrett, D.M., Bunin, N.J., Chew, A., Gonzalez, V.E., Zheng, Z., Lacey, S.F., et al. (2014). Chimeric antigen receptor T cells for sustained remissions in leukemia. N. Engl. J. Med. 371, 1507–1517.

3. Davila, M.L., Riviere, I., Wang, X., Bartido, S., Park, J., Curran, K., Chung, S.S., Stefanski, J., Borquez-Ojeda, O., Olszewska, M., et al. (2014). Efficacy and toxicity management of 19-28z CAR T cell therapy in B cell acute lymphoblastic leukemia. Sci. Transl. Med. 6, 224ra25.

4. Lee, D.W., Kochenderfer, J.N., Stetler-Stevenson, M., Cui, Y.K., Delbrook, C., Feldman, S.A., Fry, T.J., Orentas, R., Sabatino, M., Shah, N.N., et al. (2015). T cells expressing CD19 chimeric antigen receptors for acute lymphoblastic leukaemia in children and young adults: a phase 1 dose-escalation trial. Lancet 385, 517–528.

5. D'souza, N., Rossignoli, F., Golinelli, G., Grisendi, G., Spano, C., Candini, O., Osturu, S., Catani, F., Paolucci, P., Horwitz, E.M., and Dominici, M. (2015). Mesenchymal stem/stromal cells as a delivery platform in cell and gene therapies. BMC Med. 13, 186.

6. Suresh, S.C., Selvaraju, V., Thirunavukkarasu, M., Goldman, J.W., Husain, A., Alexander Palesty, J., Sanchez, J.A., McFadden, D.W., and Maulik, N. (2015). Thioredoxin-1 (Trx1) engineered mesenchymal stem cell therapy increased pro-angiogenic factors, reduced fibrosis and improved heart function in the infarcted rat myocardium. Int. J. Cardiol. 201, 517–528.

7. Cheng, Z., Ou, L., Zhou, X., Li, F., Jia, X., Zhang, Y., Liu, X., Li, Y., Ward, C.A., Melo, L.G., and Kong, D. (2008). Targeted migration of mesenchymal stem cells modified with CXCR4 gene to infarcted myocardium improves cardiac performance. Mol. Ther. 16, 571–579.

8. van Velthoven, C.T., Braccioli, L., Willemen, H.L., Kavelaars, A., and Heijnen, C.J. (2014). Therapeutic potential of genetically modified mesenchymal stem cells after neonatal hypoxic-ischemic brain damage. Mol. Ther. 22, 645–654.

9. Sage, E.K., Kolluri, K.K., McNulty, K., Da Silva Lourenco, S., Kalber, T.L., Ordidge, K.L., Davies, D., Gary Lee, Y.C., Giangreco, A., and Janes, S.M. (2014). Systemic but not topical TRAIL-expressing mesenchymal stem cells reduce tumour growth in malignant mesothelioma. Thorax 69, 638–647.

10. Niess, H., Bao, Q., Conrad, C., Zischek, C., Notohamiprodjo, M., Schwab, F., Schwarz, B., Huss, R., Jauch, K.W., Nelson, P.J., and Bruns, C.J. (2011). Selective targeting of genetically engineered mesenchymal stem cells to tumor stroma microenvironments using tissue-specific suicide gene expression suppresses growth of hepatocellular carcinoma. Ann. Surg. 254, 767–774, discussion 774–775.

11. Sage, E.K., Thakrar, R.M., and Janes, S.M. (2016). Genetically modified mesenchymal stromal cells in cancer therapy. Cytotherapy 18, 1435–1445.

12. Lim, W.A. (2010). Designing customized cell signalling circuits. Nat. Rev. Mol. Cell Biol. 11, 393–403.

13. Woodsworth, D.J., and Holt, R.A. (2017). Cell-based therapeutics: making a faustian pact with biology. Trends Mol. Med. 23, 104–115.

14. Stanton, B.C., Siciliano, V., Ghodasara, A., Wroblewska, L., Clancy, K., Trefzer, A.C., Chesnut, J.D., Weiss, R., and Voigt, C.A. (2014). Systematic transfer of prokaryotic sensors and circuits to mammalian cells. ACS Synth. Biol. 3, 880–891.

15. Sadelain, M., Brentjens, R., and Rivière, I. (2013). The basic principles of chimeric antigen receptor design. Cancer Discov. 3, 388–398.

16. Roybal, K.T., Rupp, L.J., Morsut, L., Walker, W.J., McNally, K.A., Park, J.S., and Lim, W.A. (2016). Precision tumor recognition by T cells with combinatorial antigen-sensing circuits. Cell 164, 770–779.

17. Morsut, L., Roybal, K.T., Xiong, X., Gordley, R.M., Coyle, S.M., Thomson, M., and Lim, W.A. (2016). Engineering customized cell sensing and response behaviors using synthetic notch receptors. Cell 164, 780–791.

18. Kemmer, C., Gitzinger, M., Daoud-El Baba, M., Djonov, V., Stelling, J., and Fussenegger, M. (2010). Self-sufficient control of urate homeostasis in mice by a synthetic circuit. Nat. Biotechnol. 28, 355–360.

19. Ye, L., Chang, Y.H., Xiong, Q., Zhang, P., Zhang, L., Somasundaram, P., Lepley, M., Swingen, C., Su, L., Wendel, J.S., et al. (2014). Cardiac repair in a porcine model of acute myocardial infarction with human induced pluripotent stem cell-derived cardiovascular cells. Cell Stem Cell 15, 750–761.

20. Green, E.R., and Mecsas, J. (2016). Bacterial secretion systems: an overview. Microbiol. Spectr. 4, 10.1128/microbiolspec.VMBF-0012-2015.

21. Costa, T.R.D., Felisberto-Rodrigues, C., Meir, A., Prevost, M.S., Redzej, A., Trokter, M., and Waksman, G. (2015). Secretion systems in Gram-negative bacteria: structural and mechanistic insights. Nat. Rev. Microbiol. 13, 343–359.

22. Reeves, A.Z., Spears, W.E., Du, J., Tan, K.Y., Wagers, A.J., and Lesser, C.F. (2015). Engineering Escherichia coli into a protein delivery system for mammalian cells. ACS Synth. Biol. 4, 644–654.

23. Anderson, J.C., Clarke, E.J., Arkin, A.P., and Voigt, C.A. (2006). Environmentally controlled invasion of cancer cells by engineered bacteria. J. Mol. Biol. 355, 619–627.

24. Anderson, J.C., Voigt, C.A., and Arkin, A.P. (2007). Environmental signal integration by a modular AND gate. Mol. Syst. Biol. 3, 133.

25. Barry, M., and Bleackley, R.C. (2002). Cytotoxic T lymphocytes: all roads lead to death. Nat. Rev. Immunol. 2, 401–409.

26. Voskoboinik, I., Whisstock, J.C., and Trapani, J.A. (2015). Perforin and granzymes: function, dysfunction and human pathology. Nat. Rev. Immunol. 15, 388–400.

27. de Saint Basile, G., Ménasché, G., and Fischer, A. (2010). Molecular mechanisms of biogenesis and exocytosis of cytotoxic granules. Nat. Rev. Immunol. 10, 568–579.

28. Law, R.H.P., Lukoyanova, N., Voskoboinik, I., Caradoc-Davies, T.T., Baran, K., Dunstone, M.A., D'Angelo, M.E., Orlova, E.V., Coulibaly, F., Verschoor, S., et al. (2010). The structural basis for membrane binding and pore formation by lymphocyte perforin. Nature 468, 447–451.

29. Lopez, J.A., Susanto, O., Jenkins, M.R., Lukoyanova, N., Sutton, V.R., Law, R.H., Johnston, A., Bird, C.H., Bird, P.I., Whisstock, J.C., et al. (2013). Perforin forms transient pores on the target cell plasma membrane to facilitate rapid access of granzymes during killer cell attack. Blood 121, 2659–2668.

30. Thiery, J., Keefe, D., Boulant, S., Boucrot, E., Walch, M., Martinvalet, D., Goping, I.S., Bleackley, R.C., Kirchhausen, T., and Lieberman, J. (2011). Perforin pores in the endosomal membrane trigger the release of endocytosed granzyme B into the cytosol of target cells. Nat. Immunol. 12, 770–777.

31. Stinchcombe, J.C., Majorovits, E., Bossi, G., Fuller, S., and Griffiths, G.M. (2006). Centrosome polarization delivers secretory granules to the immunological synapse. Nature 443, 462–465.

32. Cartwright, A.N.R., Griggs, J., and Davis, D.M. (2014). The immune synapse clears and excludes molecules above a size threshold. Nat. Commun. 5, 5479.

33. Woodsworth, D.J., Dunsing, V., and Coombs, D. (2015). Design parameters for granzyme-mediated cytotoxic lymphocyte target-cell killing and specificity. Biophys. J. 109, 477–488.

34. Hinrichs, C.S., and Rosenberg, S.A. (2014). Exploiting the curative potential of adoptive T-cell therapy for cancer. Immunol. Rev. 257, 56–71.

35. Huang, L., Pike, D., Sleat, D.E., Nanda, V., and Lobel, P. (2014). Potential pitfalls and solutions for use of fluorescent fusion proteins to study the lysosome. PLoS One 9, e88893.

36. Montel, A.H., Morse, P.A., and Brahmi, Z. (1995). Upregulation of B7 molecules by the Epstein-Barr virus enhances susceptibility to lysis by a human NK-like cell line. Cell. Immunol. 160, 104–114.

37. Shimizu, Y., and DeMars, R. (1989). Production of human cells expressing individual transferred HLA-A,-B,-C genes using an HLA-A,-B,-C null human cell line. J. Immunol. *142*, 3320–3328.

38. Braulke, T., and Bonifacino, J.S. (2009). Sorting of lysosomal proteins. Biochim. Biophys. Acta *1793*, 605–614.

39. Saftig, P., and Klumperman, J. (2009). Lysosome biogenesis and lysosomal membrane proteins: trafficking meets function. Nat. Rev. Mol. Cell Biol. *10*, 623–635.

40. Lopez, J.A., Jenkins, M.R., Rudd-Schmidt, J.A., Brennan, A.J., Danne, J.C., Mannering, S.I., Trapani, J.A., and Voskoboinik, I. (2013). Rapid and unidirectional perforin pore delivery at the cytotoxic immune synapse. J. Immunol. *191*, 2328–2334.

41. Breitling, J., and Aebi, M. (2013). N-linked protein glycosylation in the endoplasmic reticulum. Cold Spring Harb. Perspect. Biol. *5*, a013359.

42. van Meel, E., Lee, W.S., Liu, L., Qian, Y., Doray, B., and Kornfeld, S. (2016). Multiple domains of GlcNAc-1-phosphotransferase mediate recognition of lysosomal enzymes. J. Biol. Chem. *291*, 8295–8307.

43. Warner, J.B., Thalhauser, C., Tao, K., and Sahagian, G.G. (2002). Role of N-linked oligosaccharide flexibility in mannose phosphorylation of lysosomal enzyme cathepsin L. J. Biol. Chem. *277*, 41897–41905.

44. Qian, Y., Lee, I., Lee, W.S., Qian, M., Kudo, M., Canfield, W.M., Lobel, P., and Kornfeld, S. (2010). Functions of the alpha, beta, and gamma subunits of UDP-GlcNAc:lysosomal enzyme N-acetylglucosamine-1-phosphotransferase. J. Biol. Chem. *285*, 3360–3370.

45. Waugh, S.M., Harris, J.L., Fletterick, R., and Craik, C.S. (2000). The structure of the pro-apoptotic protease granzyme B reveals the molecular determinants of its specificity. Nat. Struct. Biol. *7*, 762–765.

46. James, J.R., and Vale, R.D. (2012). Biophysical mechanism of T-cell receptor triggering in a reconstituted system. Nature *487*, 64–69.

47. Kurschus, F.C., Kleinschmidt, M., Fellows, E., Dornmair, K., Rudolph, R., Lilie, H., and Jenne, D.E. (2004). Killing of target cells by redirected granzyme B in the absence of perforin. FEBS Lett. *562*, 87–92.

48. Gupta, R., and Brunak, S. (2002). Prediction of glycosylation across the human proteome and the correlation to protein function. Pac. Symp. Biocomput. *2002*, 310–322.

49. Blázquez, M., and Shennan, K.I.J. (2000). Basic mechanisms of secretion: sorting into the regulated secretory pathway. Biochem. Cell Biol. *78*, 181–191.

50. Portales-Casamar, E., Swanson, D.J., Liu, L., de Leeuw, C.N., Banks, K.G., Ho Sui, S.J., Fulton, D.L., Ali, J., Amirabbasi, M., Arenillas, D.J., et al. (2010). A regulatory toolbox of MiniPromoters to drive selective expression in the brain. Proc. Natl. Acad. Sci. USA *107*, 16589–16594.

Supplemental Information

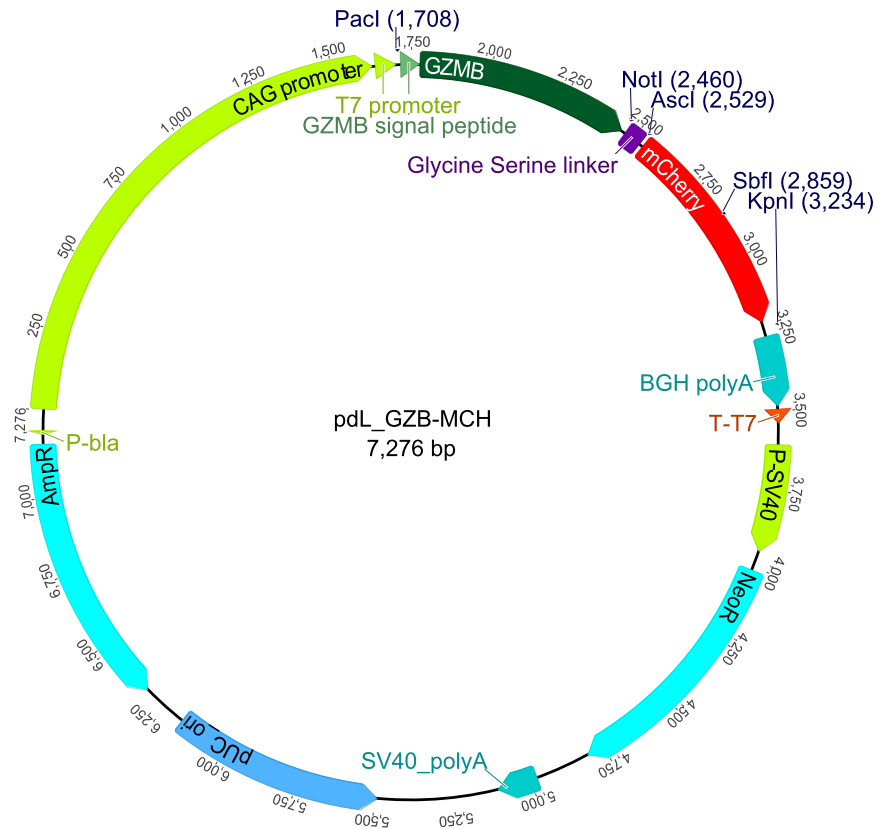**Targeted Cell-to-Cell Delivery of Protein**

Payloads via the Granzyme-Perforin Pathway

Daniel J. Woodsworth, Lisa Dreolini, Libin Abraham, and Robert A. Holt

1 Plasmids

1.1 Base pdL plasmid

Supplementary Figure 1: Base pdL vector. In this example the insert coding sequence is the granzyme B-crmCherry fusion protein (GZB-MCH). The annotations correspond to those in the genbank file.

1.2 Base pdL plasmid sequence

```
LOCUS           pdL_GZB-MCH              7276 bp     DNA      circular UNA 21-FEB-2017
DEFINITION   .
ACCESSION    .
VERSION      .
KEYWORDS     .
SOURCE
  ORGANISM
             .
FEATURES             Location/Qualifiers
     promoter        2..1628
                     /label="CAG promoter"
     promoter        1635..1702
                     /label="T7 promoter"
     sig_peptide     1717..1776
                     /gene="GZMB"
                     /label="GZMB signal peptide"
     mat_peptide     1777..2457
                     /gene="GZMB"
                     /product="granzyme B"
                     /label="GZMB"
     misc_feature    2467..2526
                     /note="Geneious type: polylinker"
                     /label="Glycine Serine linker"
     CDS             2536..3216
                     /label="mCherry"
     polyA_signal    3262..3486
                     /label="BGH polyA"
     terminator      3495..3538
                     /label="T-T7"
     promoter        3606..3949
                     /label="P-SV40"
     misc_feature    4011..4805
                     /note="Geneious type: Marker"
                     /label="NeoR"
     polyA_signal    4979..5109
                     /label="SV40_polyA"
     misc_feature    complement(5492..6162)
                     /note="Geneious type: Origin of Replication"
                     /label="pUC_ori"
     misc_feature    complement(6307..7167)
                     /note="Geneious type: Marker"
                     /label="AmpR"
     promoter        complement(7202..7208)
                     /label="P-bla"
ORIGIN
        1 ctgcaggcgt tacataactt acggtaaatg gcccgcctgg ctgaccgccc aacgaccccc
       61 gcccattgac gtcaataatg acgtatgttc ccatagtaac gccaataggg actttccatt
      121 gacgtcaatg ggtggagtat ttacggtaaa ctgcccactt ggcagtacat caagtgtatc
      181 atatgccaag tacgccccct attgacgtca atgacggtaa atggcccgcc tggcattatg
      241 cccagtacat gaccttatgg gactttccta cttggcagta catctacgta ttagtcatcg
      301 ctattaacat ggtcgaggtg agccccacgt tctgcttcac tctccccatc tcccccccct
      361 ccccaccccc aattttgtat ttatttattt tttaattatt ttgtgcagcg atggggcgg
      421 ggggggggg ggggcgcgcg ccaggcgggg cggggcgggg cgaggggcgg ggcggggcga
      481 ggcggagagg tgcggcggca gccaatcaga gcggcgcgct ccgaaagttt cctttttatgg
      541 cgaggcggcg gcggcggcgg ccctataaaa agcgaagcgc gcggcgggcg gggagtcgct
```

```
 601 gcgacgctgc  cttcgccccg  tgccccgctc  cgccgccgcc  tcgcgccgcc  cgccccggct
 661 ctgactgacc  gcgttactcc  cacaggtgag  cgggcgggac  ggcccttctc  ctccgggctg
 721 taattagcgc  ttggtttaat  gacggcttgt  ttcttttctg  tggctgcgtg  aaagccttga
 781 ggggctccgg  gagggccctt  tgtgcggggg  gagcggctcg  gggggtgcgt  gcgtgtgtgt
 841 gtgcgtgggg  agcgccgcgt  gcggctccgc  gctgcccggc  ggctgtgagc  gctgcgggcg
 901 cggcgcgggg  ctttgtgcgc  tccgcagtgt  gcgcgagggg  agcgcggccg  ggggcggtgc
 961 cccgcggtgc  ggggggggct  gcgaggggaa  caaaggctgc  gtgcggggtg  tgtgcgtggg
1021 ggggtgagca  gggggtgtgg  gcgcgtcggt  cgggctgcaa  cccccctgc   accccctcc
1081 ccgagttgct  gagcacggcc  cggcttcggg  tgcggggctc  cgtacggggc  gtggcgcggg
1141 gctcgccgtg  ccgggcgggg  ggtggcggca  ggtggggggtg  ccgggcgggg  cggggccgcc
1201 tcgggccggg  gagggctcgg  gggaggggcg  cggcggcccc  cggagcgccg  gcggctgtcg
1261 aggcgcggcg  agccgcagcc  attgcctttt  atggtaatcg  tgcgagaggg  cgcagggact
1321 tcctttgtcc  caaatctgtg  cggagccgaa  atctgggagg  cgccgccgca  cccctctag
1381 cgggcgcggg  gcgaagcggt  gcggcgccgg  caggaaggaa  atgggcgggg  agggccttcg
1441 tgcgtcgccg  cgccgccgtc  cccttctccc  tctccagcct  cggggctgtc  cgcgggggga
1501 cggctgcctt  cggggggggac  ggggcagggc  ggggttcggc  ttctggcgtg  tgaccggcgg
1561 ctctagacaa  ttgtactaac  cttcttctct  ttcctctcct  gacaggttgg  tgtacagtag
1621 cttccaccac  cggttaatac  gactcactat  aggctagcat  ttaggtgaca  ctatagaata
1681 caagctactt  gttcttttttg  cattaattaa  gccgccatgc  aaccaatcct  gcttctgctg
1741 gccttcctcc  tgctgcccag  ggcagatgca  ggggagatca  tcggggggaca  tgaggccaag
1801 ccccactccc  gcccctacat  ggcttatctt  atgatctggg  atcagaagtc  tctgaagagg
1861 tgcggtggct  tcctgatacg  agacgacttc  gtgctgacag  ctgctcactg  ttggggaagc
1921 tccataaatg  tcaccttggg  ggcccacaat  atcaaagaac  aggagccgac  ccagcagttt
1981 atccctgtga  aaagacccat  cccccatcca  gcctataatc  ctaagaactt  ctccaacgac
2041 atcatgctac  tgcagctgga  gagaaaggcc  aagcggacca  gagctgtgca  gcccctcagg
2101 ctacctagca  acaaggccca  ggtgaagcca  gggcagacat  gcagtgtggc  cggctggggg
2161 cagacggccc  ccctgggaaa  acactcacac  acactacaag  aggtgaagat  gacagtgcag
2221 gaagatcgaa  agtgcgaatc  tgacttacgc  cattattacg  acagtaccat  tgagttgtgc
2281 gtgggggacc  cagagattaa  aaagacttcc  tttaagggag  actctggagg  ccctcttgtg
2341 tgtaacaagg  tggcccaggg  cattgtctcc  tatggacgaa  acaatggcat  gcctccacga
2401 gcctgcacca  aagtctcaag  ctttgtacac  tggataaaga  aaaccatgaa  acgctacgcg
2461 gccgctggag  gtgggggttc  tggcgggggt  ggatcagggg  gtggaggttc  cggtggaggt
2521 gggtcgggcg  cgcccatcat  caaggagttc  atgcgcttca  aggtgcacat  ggagggctcc
2581 gtgaacggcc  acgagttcga  gatcgagggc  gagggcgagg  gccgccccta  cgagggcacc
2641 cagaccgcca  agctgaaggt  gaccaaggt   ggccccctgc  ccttcgcctg  ggacatcctg
2701 tcccctcagt  tcatgtacgg  ctccaaggcc  tacgtgaagc  accccgccga  catccccgac
2761 tacttgaagc  tgtccttccc  cgagggcttc  aagtgggagc  gcgtgatgaa  cttcgaggac
2821 ggcggcgtgg  tgaccgtgac  ccaggactcc  tccctgcagg  acggcgagtt  catctacaag
2881 gtgaagctgc  gcggcaccaa  cttcccctcc  gacggccccg  taatgcagaa  gaagaccatg
2941 ggctgggagg  cctcctccga  gcggatgtac  cccgaggacg  gcgccctgaa  gggcgagatc
3001 aagcagaggc  tgaagctgaa  ggacggcggc  cactacgacg  ctgaggtcaa  gaccacctac
3061 aaggccaaga  agcccgtgca  gctgcccggc  gcctacaacg  tcaacatcaa  gttggacatc
3121 acctcccaca  acgaggacta  caccatcgtg  gaacagtacg  aacgcgccga  gggccgccac
3181 tccaccggcg  gcatggacga  gctgtacaag  gaattctaat  agctcgaggg  taccactagt
3241 tagcccgctg  atcagcctcg  actgtgcctt  ctagttgcca  gccatctgtt  gtttgcccct
3301 ccccccgtgcc  ttccttgacc  ctggaaggtg  ccactcccac  tgtcctttcc  taataaaatg
3361 aggaaattgc  atcgcattgt  ctgagtaggt  gtcattctat  tctggggggt  ggggtggggc
3421 aggacagcaa  ggggggaggat  tgggaagaca  atagcaggca  tgctggggat  gcggtgggct
3481 ctatggtaac  gcgtataacc  ccttgaggcc  tctaaacggg  tcttgagggg  tttttttgact
3541 cgagcgattt  cggcctattg  gttaaaaaat  gagctgattt  aacaaaaatt  taacgcgaat
3601 taattctgtg  gaatgtgtgt  cagttagggt  gtggaaagtc  cccaggctcc  ccagcaggca
3661 gaagtatgca  aagcatgcat  ctcaattagt  cagcaaccag  gtgtggaaag  tccccaggct
3721 ccccagcagg  cagaagtatg  caaagcatgc  atctcaatta  gtcagcaacc  atagtcccgc
3781 ccctaactcc  gcccatcccg  cccctaactc  cgcccagttc  cgcccattct  ccgccccatg
3841 gctgactaat  tttttttatt  tatgcagagg  ccgaggccgc  ctctgcctct  gagctattcc
3901 agaagtagtg  aggaggcttt  tttggaggcc  taggcttttg  caaaaagctc  ccgggagctt
3961 gtatatccat  tttcggatct  gatcaagaga  caggatgagg  atcgtttcgc  atgattgaac
```

4

```
4021 aagatggatt gcacgcaggt tctccggccg cttgggtgga gaggctattc ggctatgact
4081 gggcacaaca gacaatcggc tgctctgatg ccgccgtgtt ccggctgtca gcgcaggggc
4141 gcccggttct ttttgtcaag accgacctgt ccggtgccct gaatgaactg caggacgagg
4201 cagcgcggct atcgtggctg gccacgacgg gcgttccttg cgcagctgtg ctcgacgttg
4261 tcactgaagc gggaagggac tggctgctat tgggcgaagt gccggggcag gatctcctgt
4321 catctcacct tgctcctgcc gagaaagtat ccatcatggc tgatgcaatg cggcggctgc
4381 atacgcttga tccggctacc tgcccattcg accaccaagc gaaacatcgc atcgagcgag
4441 cacgtactcg gatggaagcc ggtcttgtcg atcaggatga tctggacgaa gagcatcagg
4501 ggctcgcgcc agccgaactg ttcgccaggc tcaaggcgcg catgcccgac ggcgaggatc
4561 tcgtcgtgac ccatggcgat gcctgcttgc cgaatatcat ggtggaaaat ggccgctttt
4621 ctggattcat cgactgtggc cggctgggtg tggcggaccg ctatcaggac atagcgttgg
4681 ctacccgtga tattgctgaa gagcttggcg gcgaatgggc tgaccgcttc ctcgtgcttt
4741 acggtatcgc cgctcccgat tcgcagcgca tcgccttcta tcgccttctt gacgagttct
4801 tctgagcggg actctggggt tcgaaatgac cgaccaagcg acgcccaacc tgccatcacg
4861 agatttcgat tccaccgccg ccttctatga aaggttgggc ttcggaatcg ttttccggga
4921 cgccggctgg atgatcctcc agcgcgggga tctcatgctg gagttcttcg cccaccccaa
4981 cttgtttatt gcagcttata atggttacaa ataaagcaat agcatcacaa atttcacaaa
5041 taaagcattt ttttcactgc attctagttg tggtttgtcc aaactcatca atgtatctta
5101 tcatgtctgt ataccgtcga cctctagcta gagcttggcg taatcatggt catagctgtt
5161 tcctgtgtga aattgttatc cgctcacaat tccacacaac atacgagccg gaagcataaa
5221 gtgtaaagcc tggggtgcct aatgagtgag ctaactcaca ttaattgcgt tgcgctcact
5281 gcccgctttc cagtcgggaa acctgtcgtg ccagctgcat taatgaatcg gccaacgcgc
5341 ggggagaggc ggtttgcgta ttgggcgctc ttccgcttcc tcgctcactg actcgctgcg
5401 ctcggtcgtt cggctgcggc gagcggtatc agctcactca aaggcggtaa tacggttatc
5461 cacagaatca ggggataacg caggaaagaa catgtgagca aaaggccagc aaaaggccag
5521 gaaccgtaaa aaggccgcgt tgctggcgtt tttccatagg ctccgccccc ctgacgagca
5581 tcacaaaaat cgacgctcaa gtcagaggtg gcgaaacccg acaggactat aaagatacca
5641 ggcgtttccc cctggaagct ccctcgtgcg ctctcctgtt ccgaccctgc cgcttaccgg
5701 atacctgtcc gcctttctcc cttcgggaag cgtggcgctt tctcatagct cacgctgtag
5761 gtatctcagt tcggtgtagg tcgttcgctc caagctgggc tgtgtgcacg aacccccccgt
5821 tcagcccgac cgctgcgcct tatccggtaa ctatcgtctt gagtccaacc cggtaagaca
5881 cgacttatcg ccactggcag cagccactgg taacaggatt agcagagcga ggtatgtagg
5941 cggtgctaca gagttcttga agtggtggcc taactacggc tacactagaa gaacagtatt
6001 tggtatctgc gctctgctga agccagttac cttcggaaaa agagttggta gctcttgatc
6061 cggcaaacaa accaccgctg gtagcggttt ttttgtttgc aagcagcaga ttacgcgcag
6121 aaaaaaagga tctcaagaag atcctttgat cttttctacg gggtctgacg ctcagtggaa
6181 cgaaaactca cgttaaggga ttttggtcat gagattatca aaaaggatct tcacctagat
6241 ccttttaaat taaaaatgaa gttttaaatc aatctaaagt atatatgagt aaacttggtc
6301 tgacagttac caatgcttaa tcagtgaggc acctatctca gcgatctgtc tatttcgttc
6361 atccatagtt gcctgactcc ccgtcgtgta gataactacg atacgggagg gcttaccatc
6421 tggccccagt gctgcaatga taccgcgaga cccacgctca ccggctccag atttatcagc
6481 aataaaccag ccagccggaa gggccgagcg cagaagtggt cctgcaactt tatccgcctc
6541 catccagtct attaattgtt gccgggaagc tagagtaagt agttcgccag ttaatagttt
6601 gcgcaacgtt gttgccattg ctacaggcat cgtggtgtca cgctcgtcgt ttggtatggc
6661 ttcattcagc tccggttccc aacgatcaag gcgagttaca tgatccccca tgttgtgcaa
6721 aaaagcggtt agctccttcg gtcctccgat cgttgtcaga agtaagttgg ccgcagtgtt
6781 atcactcatg gttatggcag cactgcataa ttctcttact gtcatgccat ccgtaagatg
6841 cttttctgtg actggtgagt actcaaccaa gtcattctga gaatagtgta tgcggcgacc
6901 gagttgctct gcccggcgt caatacggga taataccgcg ccacatagca gaactttaaa
6961 agtgctcatc attggaaaac gttcttcggg gcgaaaactc tcaaggatct taccgctgtt
7021 gagatccagt tcgatgtaac ccactcgtgc acccaactga tcttcagcat cttttacttt
7081 caccagcgtt tctgggtgag caaaaacagg aaggcaaaat gccgcaaaaa agggaataag
7141 ggcgacacgg aaatgttgaa tactcatact cttccttttt caatattatt gaagcattta
7201 tcagggttat tgtctcatga gcggatacat atttgaatgt atttagaaaa ataaacaaat
7261 aggggttccg cgagct
//
```

5

1.3 Coding sequence inserts

Coding sequences listed below extend from the PacI site to KpnI site of the pdL vector.

>GZB1–MCH
TTAATTAAGCCGCCATGCAACCAATCCTGCTTCTGCTGGCCTTCCTCCTGCTGCCCAGGGCAGATGCAATCATCGGGGGA
CATGAGGCCAAGCCCCACTCCCGCCCCTACATGGCTTATCTTATGATCTGGGATCAGAAGTCTCTGAAGAGGTGCGGTGG
CTTCCTGATACGAGACGACTTCGTGCTGACAGCTGCTCACTGTTGGGGAAGCTCCATAAATGTCACCTTGGGGGCCCACA
ATATCAAAGAACAGGAGCCGACCCAGCAGTTTATCCCTGTGAAAAGACCCATCCCCCATCCAGCCTATAATCCTAAGAAC
TTCTCCAACGACATCATGCTACTGCAGCTGGAGAGAAAGGCCAAGCGGACCAGAGCTGTGCAGCCCCTCAGGCTACCTAG
CAACAAGGCCCAGGCGGCCGCTGGAGGTGGGGGTTCTGGCGGGGGTGGATCAGGGGGTGGAGGTTCCGGTGGAGGTGGGT
CGGGCGCGCCCATCATCAAGGAGTTCATGCGCTTCAAGGTGCACATGGAGGGCTCCGTGAACGGCCACGAGTTCGAGATC
GAGGGCGAGGGCGAGGGCCGCCCCTACGAGGGCACCCAGACCGCCAAGCTGAAGGTGACCAAGGGTGGCCCCCTGCCCTT
CGCCTGGGACATCCTGTCCCCTCAGTTCATGTACGGCTCCAAGGCCTACGTGAAGCACCCCGCCGACATCCCCGACTACT
TGAAGCTGTCCTTCCCCGAGGGCTTCAAGTGGGAGCGCGTGATGAACTTCGAGGACGGCGGCGTGGTGACCGTGACCCAG
GACTCCTCCCTGCAGGACGGCGAGTTCATCTACAAGGTGAAGCTGCGCGGCACCAACTTCCCCTCCGACGGCCCCGTAAT
GCAGAAGAAGACCATGGGCTGGGAGGCCTCCTCCGAGCGGATGTACCCCGAGGACGGCGCCCTGAAGGGCGAGATCAAGC
AGAGGCTGAAGCTGAAGGACGGCGGCCACTACGACGCTGAGGTCAAGACCACCTACAAGGCCAAGAAGCCCGTGCAGCTG
CCCGGCGCCTACAACGTCAACATCAAGTTGGACATCACCTCCCACAACGAGGACTACACCATCGTGGAACAGTACGAACG
CGCCGAGGGCCGCCACTCCACCGGCGGCATGGACGAGCTGTACAAGGAATTCTAATAGCTCGAGGGTACC
>GZB2–MCH
TTAATTAAGCCGCCATGCAACCAATCCTGCTTCTGCTGGCCTTCCTCCTGCTGCCCAGGGCAGATGCAGTGAAGCCAGGG
CAGACATGCAGTGTGGCCGGCTGGGGGCAGACGGCCCCCCTGGGAAAACACTCACACACACTACAAGAGGTGAAGATGAC
AGTGCAGGAAGATCGAAAGTGCGAATCTGACTTACGCCATTATTACGACAGTACCATTGAGTTGTGCGTGGGGGACCCAG
AGATTAAAAAGACTTCCTTTAAGGGGGACTCTGGAGGCCCTCTTGTGTGTAACAAGGTGGCCCAGGGCATTGTCTCCTAT
GGACGAAACAATGGCATGCCTCCACGAGCCTGCACCAAAGTCTCAAGCTTTGTACACTGGATAAAGAAAACCATGAAACG
CTACGCGGCCGCTGGAGGTGGGGGTTCTGGCGGGGGTGGATCAGGGGGTGGAGGTTCCGGTGGAGGTGGGTCGGGCGCGC
CCATCATCAAGGAGTTCATGCGCTTCAAGGTGCACATGGAGGGCTCCGTGAACGGCCACGAGTTCGAGATCGAGGGCGAG
GGCGAGGGCCGCCCCTACGAGGGCACCCAGACCGCCAAGCTGAAGGTGACCAAGGGTGGCCCCCTGCCCTTCGCCTGGGA
CATCCTGTCCCCTCAGTTCATGTACGGCTCCAAGGCCTACGTGAAGCACCCCGCCGACATCCCCGACTACTTGAAGCTGT
CCTTCCCCGAGGGCTTCAAGTGGGAGCGCGTGATGAACTTCGAGGACGGCGGCGTGGTGACCGTGACCCAGGACTCCTCC
CTGCAGGACGGCGAGTTCATCTACAAGGTGAAGCTGCGCGGCACCAACTTCCCCTCCGACGGCCCCGTAATGCAGAAGAA
GACCATGGGCTGGGAGGCCTCCTCCGAGCGGATGTACCCCGAGGACGGCGCCCTGAAGGGCGAGATCAAGCAGAGGCTGA
AGCTGAAGGACGGCGGCCACTACGACGCTGAGGTCAAGACCACCTACAAGGCCAAGAAGCCCGTGCAGCTGCCCGGCGCC
TACAACGTCAACATCAAGTTGGACATCACCTCCCACAACGAGGACTACACCATCGTGGAACAGTACGAACGCGCCGAGGG
CCGCCACTCCACCGGCGGCATGGACGAGCTGTACAAGGAATTCTAATAGCTCGAGGGTACC
>GZB–MCH
TTAATTAAGCCGCCATGCAACCAATCCTGCTTCTGCTGGCCTTCCTCCTGCTGCCCAGGGCAGATGCAGGGGGAGATCATC
GGGGGACATGAGGCCAAGCCCCACTCCCGCCCCTACATGGCTTATCTTATGATCTGGGATCAGAAGTCTCTGAAGAGGTG
CGGTGGCTTCCTGATACGAGACGACTTCGTGCTGACAGCTGCTCACTGTTGGGGAAGCTCCATAAATGTCACCTTGGGGG
CCCACAATATCAAAGAACAGGAGCCGACCCAGCAGTTTATCCCTGTGAAAAGACCCATCCCCCATCCAGCCTATAATCCT
AAGAACTTCTCCAACGACATCATGCTACTGCAGCTGGAGAGAAAGGCCAAGCGGACCAGAGCTGTGCAGCCCCTCAGGCT
ACCTAGCAACAAGGCCCAGGTGAAGCCAGGGCAGACATGCAGTGTGGCCGGCTGGGGGCAGACGGCCCCCCTGGGAAAAC
ACTCACACACACTACAAGAGGTGAAGATGACAGTGCAGGAAGATCGAAAGTGCGAATCTGACTTACGCCATTATTACGAC
AGTACCATTGAGTTGTGCGTGGGGGACCCAGAGATTAAAAAGACTTCCTTTAAGGGGGACTCTGGAGGCCCTCTTGTGTG
TAACAAGGTGGCCCAGGGCATTGTCTCCTATGGACGAAACAATGGCATGCCTCCACGAGCCTGCACCAAAGTCTCAAGCT
TTGTACACTGGATAAAGAAAACCATGAAACGCTACGCGGCCGCTGGAGGTGGGGGTTCTGGCGGGGGTGGATCAGGGGGT
GGAGGTTCCGGTGGAGGTGGGTCGGGCGCGCCCATCATCAAGGAGTTCATGCGCTTCAAGGTGCACATGGAGGGCTCCGT
GAACGGCCACGAGTTCGAGATCGAGGGCGAGGGCGAGGGCCGCCCCTACGAGGGCACCCAGACCGCCAAGCTGAAGGTGA
CCAAGGGTGGCCCCCTGCCCTTCGCCTGGGACATCCTGTCCCCTCAGTTCATGTACGGCTCCAAGGCCTACGTGAAGCAC
CCCGCCGACATCCCCGACTACTTGAAGCTGTCCTTCCCCGAGGGCTTCAAGTGGGAGCGCGTGATGAACTTCGAGGACGG
CGGCGTGGTGACCGTGACCCAGGACTCCTCCCTGCAGGACGGCGAGTTCATCTACAAGGTGAAGCTGCGCGGCACCAACT
TCCCCTCCGACGGCCCCGTAATGCAGAAGAAGACCATGGGCTGGGAGGCCTCCTCCGAGCGGATGTACCCCGAGGACGGC
GCCCTGAAGGGCGAGATCAAGCAGAGGCTGAAGCTGAAGGACGGCGGCCACTACGACGCTGAGGTCAAGACCACCTACAA
GGCCAAGAAGCCCGTGCAGCTGCCCGGCGCCTACAACGTCAACATCAAGTTGGACATCACCTCCCACAACGAGGACTACA
CCATCGTGGAACAGTACGAACGCGCCGAGGGCCGCCACTCCACCGGCGGCATGGACGAGCTGTACAAGGAATTCTAATAG

```
CTCGAGGGTACC
>GZBSS–MCH
TTAATTAAGCCGCCATGCAACCGATCTTGTTGCTGCTGGCTTTTCTGCTGTTGCCAAGGGCAGACGCTGGAGAGGGCGCG
CCCATCATCAAGGAGTTCATGCGCTTCAAGGTGCACATGGAGGGCTCCGTGAACGGCCACGAGTTCGAGATCGAGGGCGA
GGGCGAGGGCCGCCCCTACGAGGGCACCCAGACCGCCAAGCTGAAGGTGACCAAGGGTGGCCCCCTGCCCTTCGCCTGGG
ACATCCTGTCCCCTCAGTTCATGTACGGCTCCAAGGCCTACGTGAAGCACCCCGCCGACATCCCCGACTACTTGAAGCTG
TCCTTCCCCGAGGGCTTCAAGTGGGAGCGCGTGATGAACTTCGAGGACGGCGGCGTGGTGACCGTGACCCAGGACTCCTC
CCTGCAGGACGGCGAGTTCATCTACAAGGTGAAGCTGCGCGGCACCAACTTCCCCTCCGACGGCCCCGTAATGCAGAAGA
AGACCATGGGCTGGGAGGCCTCCTCCGAGCGGATGTACCCCGAGGACGGCGCCCTGAAGGGCGAGATCAAGCAGAGGCTG
AAGCTGAAGGACGGCGGCCACTACGACGCTGAGGTCAAGACCACCTACAAGGCCAAGAAGCCCGTGCAGCTGCCCGGCGC
CTACAACGTCAACATCAAGTTGGACATCACCTCCCACAACGAGGACTACACCATCGTGGAACAGTACGAACGCGCCGAGG
GCCGCCACTCCACCGGCGGCATGGACGAGCTGTACAAGGAATTCTAATAGCTCGAGGGTACC
>GZBSS–MCH–GZBSM
TTAATTAAGCCGCCATGCAACCGATCTTGTTGCTGCTGGCTTTTCTGCTGTTGCCAAGGGCAGACGCTGGAGAGGGCGCG
CCCATCATCAAGGAGTTCATGCGCTTCAAGGTGCACATGGAGGGCTCCGTGAACGGCCACGAGTTCGAGATCGAGGGCGA
GGGCGAGGGCCGCCCCTACGAGGGCACCCAGACCGCCAAGCTGAAGGTGACCAAGGGTGGCCCCCTGCCCTTCGCCTGGG
ACATCCTGTCCCCTCAGTTCATGTACGGCTCCAAGGCCTACGTGAAGCACCCCGCCGACATCCCCGACTACTTGAAGCTG
TCCTTCCCCGAGGGCTTCAAGTGGGAGCGCGTGATGAACTTCGAGGACGGCGGCGTGGTGACCGTGACCCAGGACTCCTC
CCTGCAGGACGGCGAGTTCATCTACAAGGTGAAGCTGCGCGGCACCAACTTCCCCTCCGACGGCCCCGTAATGCAGAAGA
AGACCATGGGCTGGGAGGCCTCCTCCGAGCGGATGTACCCCGAGGACGGCGCCCTGAAGGGCGAGATCAAGCAGAGGCTG
AAGCTGAAGGACGGCGGCCACTACGACGCTGAGGTCAAGACCACCTACAAGGCCAAGAAGCCCGTGCAGCTGCCCGGCGC
CTACAACGTCAACATCAAGTTGGACATCACCTCCCACAACGAGGACTACACCATCGTGGAACAGTACGAACGCGCCGAGG
GCCGCCACTCCACCGGCGGCATGGACGAGCTGTACAAGGAATTCACAGCTGCTCACTGTTGGGGAAGCTCCATAAATGTC
ACCTTGGGGGCCCACAATATCAAAGAACAGGAGCCGACCCAGCAGTTTATCCCTGTGAAAAGACCCATCCCCCATCCAGC
CTATAATCCTAAGAACTTCTCCAACGACATCATGCTACTGCAGCTGGAGAGAAAGGGTACC
>MCH
TTAATTAAGCCGCCATGATCATCAAGGAGTTCATGCGCTTCAAGGTGCACATGGAGGGCTCCGTGAACGGCCACGAGTTC
GAGATCGAGGGCGAGGGCGAGGGCCGCCCCTACGAGGGCACCCAGACCGCCAAGCTGAAGGTGACCAAGGGTGGCCCCCT
GCCCTTCGCCTGGGACATCCTGTCCCCTCAGTTCATGTACGGCTCCAAGGCCTACGTGAAGCACCCCGCCGACATCCCCG
ACTACTTGAAGCTGTCCTTCCCCGAGGGCTTCAAGTGGGAGCGCGTGATGAACTTCGAGGACGGCGGCGTGGTGACCGTG
ACCCAGGACTCCTCCCTGCAGGACGGCGAGTTCATCTACAAGGTGAAGCTGCGCGGCACCAACTTCCCCTCCGACGGCCC
CGTAATGCAGAAGAAGACCATGGGCTGGGAGGCCTCCTCCGAGCGGATGTACCCCGAGGACGGCGCCCTGAAGGGCGAGA
TCAAGCAGAGGCTGAAGCTGAAGGACGGCGGCCACTACGACGCTGAGGTCAAGACCACCTACAAGGCCAAGAAGCCCGTG
CAGCTGCCCGGCGCCTACAACGTCAACATCAAGTTGGACATCACCTCCCACAACGAGGACTACACCATCGTGGAACAGTA
CGAACGCGCCGAGGGCCGCCACTCCACCGGCGGCATGGACGAGCTGTACAAGGAATTCTAATAGCTCGAGGGTACC
```

2   Image filtration and colocalization analysis: `MATLAB` source code

```matlab
%————————————————————————————————%
%——Name: LAGfilter_batch.m
%——Author: Daniel Woodsworth
%——Date: March 3, 2017
%
%LAG = local and global filter
%
%Basic idea is to account for local variations in background signal, but
%also to achieve robust filtering of noise (so local and global filtering)
%
%To do this, first calculate local background for each pixel, subtract this
%background from original image.
%
```

```matlab
%Then calculate global median absolute devation. Use this as estimate of
%variance of pixel noise, and define threshold as some multiple of this.
%Define all pixels below this threshold as noise, and set to zero.

%Local pixel intensity idea comes from Dunn et al 2011
%Median absolute deviation idea comes from Josh Scurl

 clear all
 close all
 clc

%#####PARAM SET HERE######
%Set paths here for input and output directories
 inPath = '/Volumes/DAN/coloc/RAW/';
 outPath = '/Volumes/DAN/coloc/FILT/';

%#####PARAM SET HERE######
%length on either side of current pixel that to make box for median
%calculation
 L = 12;

%#####PARAM SET HERE######
%Number of standard deviations above MAD to consider as above backcground
%These are empirical
 C0_threshold = 3;
 C1_threshold = 6;

%#####PARAM SET HERE######
%Regex pattern for extracting unique identifier of sample image (e.g.
%within given sample, whatever IDs the actual image files)
 CaptureNumberPattern = '^Capture_(\d+)_';


%Get directories in basepath
 tmp = dir(inPath);
 dirs = {tmp.name};
 dirs([1,2]) = []; %Delete . and ..

 for dirindex = 1:length(dirs)

    %Assume each directory name is sample name
    SampleName = dirs{dirindex};
    path = fullfile(inPath, dirs{dirindex});
    writePath = fullfile(outPath, dirs{dirindex});


    %Get all image file names, assuming tiff extension
    im_files = dir(fullfile(path,'*.tiff'));
    fnames = {im_files.name};

    %Get all unique captures. Each capture has separate tiff for each
    %channel. Assume format of Name_Cx.tiff, where x = 0,1 is channel id.
    %Strip channel id to get actual name, then strip duplicates.
    [temp, basenames, extensions] = cellfun(@fileparts,fnames,'UniformOutput', false);
    ImageNames = cellfun(@(x) x(1:end-3), basenames, 'UniformOutput', false);
    ImageNames = unique(ImageNames);
```

```matlab
mkdir(writePath);

SampleName

for i = 1:length(ImageNames)

    %Get unique identifier of image file name
    [tokens,matches] = regexp(ImageNames{i},CaptureNumberPattern,'tokens','match');
    CaptureNumber = cell2mat(tokens{1});

    CaptureNumber

    C0_img_name = fullfile(path,strcat(ImageNames{i},'_C0',extensions{1}));
    C1_img_name = fullfile(path,strcat(ImageNames{i},'_C1',extensions{1}));

    %%% Read image
    imf = imfinfo(C0_img_name);
    C0_img = zeros(imf(1).Height, imf(1).Width, 'single');
    C0_img(:,:) = imread(C0_img_name);

    imf = imfinfo(C1_img_name);
    C1_img = zeros(imf(1).Height, imf(1).Width, 'single');
    C1_img(:,:) = imread(C1_img_name);

    %------C0 = green channel = lytic granule filter ------%
    %Useful for punctuate type objects

    %min and max pixels to consider, to account for edge cases
    min_pix = L+1;
    max_pix = size(C0_img,1)-L;



    %Initialize background matrix to maximum pixel intensity
    bg = repmat(max(C0_img(:)),size(C0_img,1),size(C0_img,1));

    %Calculate localized background pixel intensity for whole image
    for k = min_pix:max_pix
        for j = min_pix:max_pix

            sub = C0_img((k-L):(k+L),(j-L):(j+L));

            bg(k,j) = median(sub(:));

        end
    end

    %Subtract local background from image
    C0_im_bgfilt = C0_img-bg;

    %Set any negative pixels to 0
    C0_im_bgfilt(C0_im_bgfilt < 0) = 0;


    %Now subtract MAD from image to filter pixel noise
    %See below for more information
    %Since so many pixels are 0, use all nonzero pixels to calculate MAD
```

```matlab
%I don't know why using the original image works better, but it cleans up
%pixel noise better (essentially a higher threshold)

C0_pos = C0_img(C0_img > 0);
mad_C0 = median(abs(C0_pos(:) - median(C0_pos(:))));
noise_std_C0 = 1.4826 * mad_C0; %See below for explanation

%Noise filter. Set all pixels below threshold to 0
C0_mad_sub = C0_im_bgfilt;

C0_mad_sub(C0_mad_sub < noise_std_C0 * C0_threshold) = 0;


%C1 = RED = mCherry channel
%————Good for homogenous structures————%
%
%Just do MAD threshold, but with 6sigma


C1_pos = C1_img(C1_img > 0);
mad_C1 = median(abs(C1_pos(:) - median(C1_pos(:))));
noise_std_C1 = 1.4826 * mad_C1; %See below for explanation

%Noise filter. Set all pixels below 6 sigma threshold to 0
C1_mad_sub = C1_img;

C1_mad_sub(C1_mad_sub < noise_std_C1 * C1_threshold) = 0;


%Write images
C0_OUT = fullfile(writePath, strcat(ImageNames{i},'_filt_C0 ',extensions{1}));
C1_OUT = fullfile(writePath, strcat(ImageNames{i},'_filt_C1 ',extensions{1}));

imwrite(uint16(C0_mad_sub),C0_OUT);
imwrite(uint16(C1_mad_sub),C1_OUT);


    end

end

%————————Background on MAD derivation etc————%

% Convert the median absolute deviation to something more resembling a
% standard deviation.  This is used instead of calculating the standard
% deviation directly because the median absolute deviation ignores outliers
% (and actual spots), giving a result after normalisation closer to the
% standard deviation of noise alone, with other image features ignored.
% (See http://en.wikipedia.org/wiki/Median_absolute_deviation#Relation_to_standard_deviation
% for the conversion factor)

%calculate the absolute median devation
%This is mad = median(abs(Intensity_i-median(Intensity)))
```

```
%In other words: calculate median intensity of images using all pixels.
%Subtract this from each pixel.
%Take absolute value of these values
%Calculate median of these values
%
%Sigma ~1.4mad (see wikipedia article on mad)
%To be very sure that retain only signal, take all pixels that have
%intensity that is 6*sigma above 1.4*mad
```